IEEE Access
Multidisciplinary | Rapid Review | Open Access Journal

Received 8 October 2023, accepted 3 November 2023, date of publication 7 November 2023, date of current version 13 November 2023.

Digital Object Identifier 10.1109/ACCESS.2023.3330780

RESEARCH ARTICLE

Design of LDPC Coded Multi-User Massive MIMO Systems With MMSE-Based Iterative Joint Detection and Decoding

HAN JIN PARK AND JEONG WOO LEE, (Member, IEEE)
School of Electrical and Electronics Engineering, Chung-Ang University, Seoul 06974, South Korea

Corresponding author: Jeong Woo Lee (jwlee2@cau.ac.kr)

This work was supported by the Ministry of Science and ICT (MSIT), South Korea, through the Information Technology Research Center (ITRC) Support Program supervised by the Institute for Information and Communications Technology Planning and Evaluation under Grant IITP-2023-RS-2022-00156353.

ABSTRACT We design a low-density parity-check (LDPC) coded multi-user massive multiple-input multiple-output (MIMO) system to achieve a high error correcting capability with a fast convergence speed of iterative joint detection and decoding (JDD) process employing a low-complexity detection. Minimum mean squared error detection with parallel interference cancellation (MMSE-PIC) and its variations are considered as low-complexity linear detection algorithms. We provide a factor graph representation of LDPC coded multi-user massive MIMO system using JDD algorithm employing MMSE-PIC detection, and we formulate updating rules of messages flowing in the JDD process. We propose a practical and efficient tool for analyzing the extrinsic information transfer (EXIT) characteristics of messages exchanged between detector and decoder, based on which LDPC codes and JDD strategy are jointly designed to result in a low bit error rate (BER) and a fast convergence speed of JDD mechanism. It is observed that the error correcting capability and JDD convergence behavior predicted by the proposed analysis tool match well the actual performances obtained by simulations. It is also observed that LDPC coded multi-user massive MIMO system employing LDPC codes and JDD strategy designed optimally by the proposed EXIT analysis tool achieves a lower BER with a faster convergence speed.

INDEX TERMS Coded multi-user massive-MIMO, LDPC codes, joint detection and decoding, MMSE-PIC, EXIT analysis.

I. INTRODUCTION

As the demand for wireless and mobile communication services is growing at a rapid pace, research and development for communication technologies supporting high data rate and high spectral efficiency as well as serving a high number of users is strongly required. As one of promising solutions to meet these requirements, multi-input and multi-output (MIMO) technology was proposed in communication system design [1], [2], and recently, massive MIMO systems have been proposed to achieve even higher data rates in wireless communication systems [3], [4]. Through intensive investigations and studies in academia and engineering fields, the massive MIMO system is considered one of key technologies for the next generation cellular networks, known as the fifth generation (5G) systems [5], [6], [7]. Among various forms of application, a multi-user massive MIMO system, in which a base station (BS) is equipped with a massive number of antennas to serve many user equipments (UE) simultaneously, has been actively studied to be adopted in 5G systems [8], [9].

In a massive MIMO system, optimal signal detection is not feasibly implementable due to a resultant high computational complexity. Thus, low-complexity signal detection algorithms have been actively studied to make a massive MIMO technology be a viable solution in practical communication systems. As a result, suboptimal detection algorithms based on belief propagation (BP) over factor graph (FG) were

The associate editor coordinating the review of this manuscript and approving it for publication was Walid Al-Hussaibi.

proposed [10], [11]. Suboptimal linear detection algorithms including zero forcing (ZF) detection [12], [13] and minimum mean squared error (MMSE) detection [14], [15], [16] have also been intensively studied for the purpose of complexity reduction in massive MIMO systems. The parallel interference cancellation (PIC) process has been applied to MMSE-based iterative joint detection and decoding (JDD) schemes [17], [18], [19], [20], [21], which is referred to as MMSE-PIC detection. Numerical analysis technique has also been applied to iterative massive MIMO detection scheme for a complexity reduction [22], [23].

Error control coding has widely been used in various communication systems for the purpose of enhancing communication reliability, by which transmit power can be saved at the cost of bandwidth expansion. Low-density parity-check (LDPC) codes have recently been selected in various wireless or wired communication standards thanks to the capacity approaching error correction capability [24], [25], [26]. Communication standards adopting LDPC codes include IEEE802.16e (mobile WiMAX) [27], EN 302 307 (DVB-S2) [28] and IEEE802.3ca (E-PON) [29]. Density evolution algorithm enables us to design LDPC codes efficiently and analyze the behavior of iterative decoding [30], among which the extrinsic information transfer (EXIT) chart is the most well-known and extensively used example [31]. There also exist huge amount of research works that applied LDPC codes to MIMO systems for the purpose of improving transmission reliability. The design and analysis of LDPC coded MIMO system has been conducted by using the density evolution algorithm [32], [33], [34], [35].

In order to improve further the communication reliability of massive MIMO systems, it is desirable to apply LDPC codes as an error correction scheme [36], [37], [38], [39], [40], [41], [42], [43], [44]. To gain a high level of performance improvement from the LDPC coded multi-user massive MIMO system, we implement an iterative JDD mechanism in the receiver. The additional computational complexity resulting from decoding process needs to be compensated by the complexity reduction attained by using a low-complexity detection algorithm. There exist previous research works for designing LDPC codes for massive MIMO system equipped with low-complexity detection algorithm. Following are some examples. Modified MMSE and matched filter (MF) soft-output detection [45] and the FG-based BP detection with Gaussian approximation of interference (FG-GAI BP) [37], [46], [47] were considered in designing LDPC codes for massive MIMO systems. Iterative soft-input soft-output (SISO) MMSE detectors were proposed to enhance the signal detection of massive MIMO systems [17], [18], [19], [20], [21]. Protograph LDPC codes [43] and LDPC coded space shift keying were proposed for massive MIMO system with a low-complexity detector [48].

In the coded massive MIMO system, the error correction capability, the computational complexity and the convergence speed of JDD process are key issues to judge the feasibility of the overall system. Among these issues, the convergence speed of JDD is critical to meet the latency requirement, but it has not received enough attention in conventional works. The JDD process is composed of detection, decoding and message exchange between these two units. Each of detection and decoding units can have its own local iterations, and the overall round-trip process from detector to detector via decoder forms a global iteration. We can control the JDD convergence speed by the ratio of the numbers of detection local iterations and decoding local iterations in one global iteration, where this ratio will be called a JDD strategy. Then, LDPC codes are designed optimally together with selecting JDD strategy in order to achieve the desirable performance in terms of both bit error rate (BER) and JDD convergence speed. There exist few works considering JDD convergence speed when designing LDPC codes. Thus, there is a strong demand for a design tool by which we can construct coded massive MIMO system achieving both lower BER and faster JDD convergence. In the previous work of the authors [37], LDPC codes and JDD strategy are optimally designed for multi-user massive MIMO system adopting FG-GAI BP as a low-complexity detection algorithm. Linear detectors require lower complexity than FG BP based detectors, so we consider MMSE-PIC, which is widely used, and its variations as a low-complexity detection algorithm in the coded massive MIMO system. As variations of MMSE-PIC detection, we consider Approximate MMSE-PIC and Gauss-Seidel-aided MMSE-PIC algorithms. We represent the LDPC coded multi-user massive MIMO system by a factor graph composed of observation nodes, detection nodes, switch nodes, variable nodes and check nodes connected through edges. Then, we formulate message updating rules in component units of JDD process employing a low-complexity linear detection to fit in our framework. We define the EXIT characteristics of MMSE-PIC detector and its variations, and combine it with the decoder to form an overall EXIT characteristic function representing the whole JDD process.

By using the obtained EXIT characteristics, we trace the density evolution of messages flowing in JDD by which the convergence speed and BER are predicted. In EXIT analysis, BER performance can be evaluated by the threshold, meaning the value of E_b/N_0 over which BER improves abruptly. In this manner, we choose the JDD strategy to result in a fast convergence and optimize degree distributions of factor graph of LDPC codes to result in a low threshold. Then, the parity check matrix of LDPC codes is constructed by using the progressive edge growth (PEG) algorithm [49]. It is observed that the performance in terms of BER and convergence speed predicted by the proposed analysis tool is consistent with the result obtained by simulations. This observation validates that the proposed design procedure based on EXIT analysis tool is practically useful in designing coded multi-user massive MIMO systems to achieve low BER with fast JDD convergence speed. The proposed design tool can be used compatibly for any kind of detection schemes once the analysis on the detection mechanism is conducted. It is observed from simulations that optimally selected JDD

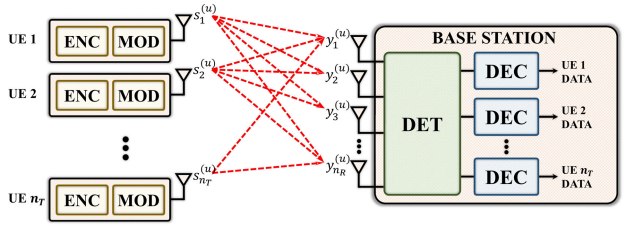

FIGURE 1. Structure of coded multi-user massive MIMO system.

strategy results in a faster convergence of JDD algorithm and consequently may satisfy the latency requirement of multi-user massive MIMO system in practical applications more easily.

This paper is organized as follows. In Sec. II, we present a system model for LDPC coded multi-user massive MIMO systems and introduce a corresponding factor graph representation. In Sec. III, we analyze MMSE-PIC detector and its variations to formulate the message updating rule in JDD process. We propose an EXIT analysis tool to investigate the behavior of JDD of the LDPC coded multi-user massive MIMO system in Sec. IV. In Sec. V, we design LDPC codes and a JDD strategy by using the proposed EXIT analysis tool to show low BER and fast JDD convergence. In Sec. VI, we evaluate BER performances of the proposed LDPC coded multi-user massive MIMO system in various points of view. Then, we confirm that the performance prediction obtained by the proposed tool is consistent with the actual simulation result. Finally, we conclude this paper in Sec. VII.

II. SYSTEM MODEL

We consider an uplink transmission of a coded multi-user massive MIMO system, in which n_T independent UEs with a single antenna transmit data to a BS equipped with n_R antennas as depicted in Fig. 1. At each UE, K information bits are encoded to N-bit codeword, resulting in a code rate of $R = K/N$, which is modulated as M-ary symbols. Then, $U = N/\log_2 M$ symbols are generated and transmitted to BS over U channel uses by each UE. Let $s_t^{(u)}$ denote a symbol transmitted by UE t at the u-th channel use, where $t = 1, 2, \cdots, n_T$ and $u = 1, 2, \ldots, U$. We let $\mathbf{s}^{(u)} = [s_1^{(u)} \cdots s_{n_T}^{(u)}]^T \in \mathcal{C}^{n_T \times 1}$ denote a symbol vector transmitted from UEs to BS at the u-th channel use, where $s_1^{(u)}, \cdots, s_{n_T}^{(u)}$ are transmitted at the same time. We also let $y_r^{(u)}$, $r = 1, \cdots, n_R$, denote a received signal by the r-th receive antenna of BS at the u-th channel use. Then, the received signal vector $\mathbf{y}^{(u)} = [y_1^{(u)} \cdots y_{n_R}^{(u)}]^T \in \mathcal{C}^{n_R \times 1}$ can be expressed as

$$\mathbf{y}^{(u)} = \mathbf{H}^{(u)}\mathbf{s}^{(u)} + \mathbf{n}^{(u)}, \qquad u = 1, 2, \ldots, U, \tag{1}$$

where $\mathbf{H}^{(u)} \in \mathcal{C}^{n_R \times n_T}$ denotes a channel gain matrix whose entries obey the independent and identically distributed (i.i.d.) complex Gaussian with zero-mean and unit-variance, and $\mathbf{n}^{(u)} = [n_1^{(u)} \cdots n_{n_R}^{(u)}]^T \in \mathcal{C}^{n_R \times 1}$ denotes an additive noise vector whose entries are i.i.d. zero-mean circular symmetric complex white Gaussian with variance of σ^2.

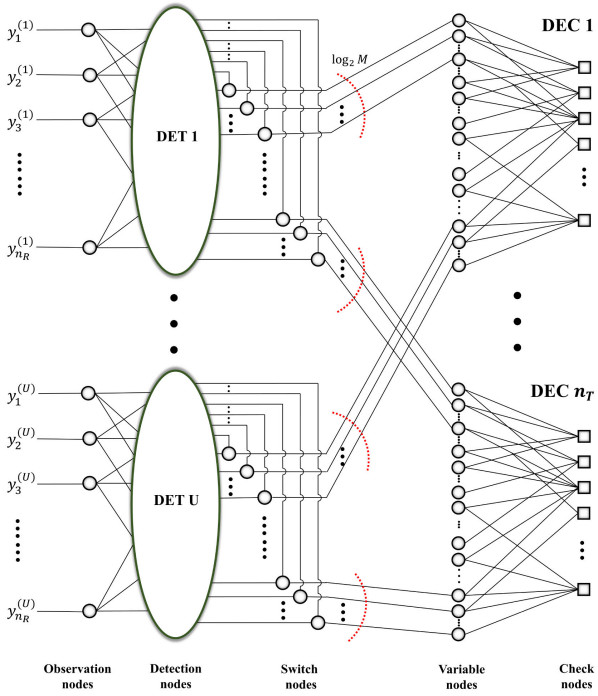

FIGURE 2. Factor graph representation for the receiver of LDPC coded multi-user massive MIMO system.

The receiver of coded multi-user massive MIMO system can be represented by a factor graph as shown in Fig. 2. There exist U detectors and n_T decoders, where each detector reflects multi-user detection performed by BS at each channel use and each decoder reflects decoding operation for data of each UE. Each detector is represented by a single detection node while each decoder consists of N variable nodes and $N - K$ check nodes. Detection nodes deliver soft information regarding code bits composing transmit symbols to corresponding variable nodes in decoders via switch nodes. Note that the t-th group of $\log_2 M$ switch nodes of the u-th detection node are connected to the u-th group of $\log_2 M$ variable nodes in the t-th decoder. Switch nodes change directions of message flows between detector and decoder. They switch their functions between i) adding incoming messages and delivering the result to a target node, and ii) passing the incoming message to a target node. Observation nodes collect received signals and input them to detection nodes.

III. JOINT DETECTION AND DECODING

For given received signals over U channel uses, the receiver performs JDD in an iterative manner over the factor graph shown in Fig.2. Iterative process can be applied to both detection and decoding. Iterative process can also be used in message exchange between detector and decoder. We call iterations inside detection and decoding as local iterations. Then we define a global iteration as the sequence of detection, message delivery from detector to decoder, decoding, and message delivery from decoder to detector. We allow multiple

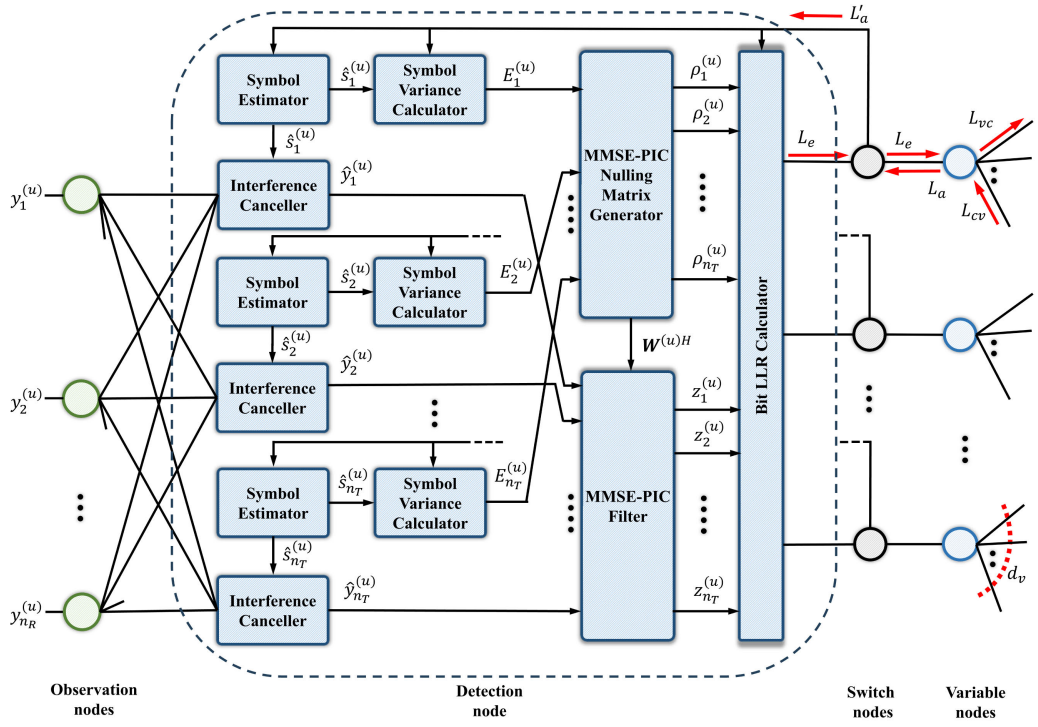

FIGURE 3. Detailed view of detection node in coded multi-user massive MIMO system.

local iterations in a global iteration, where N_{det} and N_{dec} denote numbers of local iterations inside detector and decoder, respectively. This is different from conventional schemes in which a global iteration is composed of one detection iteration and one decoding iteration. We define a JDD strategy as the ratio $N_{det} : N_{dec}$ composing one global iteration, where the ratio represents strictly two numbers N_{det} and N_{dec} themselves without allowing the cancellation of common factors. We let N_g denote the number of global iterations.

A. LOW-COMPLEXITY LINEAR DETECTION

We consider a MMSE-PIC detection and its variations as a low-complexity linear detection algorithm to be implemented in JDD of coded multi-user massive MIMO system. As variations of MMSE-PIC, we consider Approximate MMSE-PIC and Gauss-Seidel-aided MMSE-PIC to further lower the computational complexity required by JDD mechanism.

1) MMSE-PIC DETECTION

The task of MMSE-PIC detector is obtaining soft decision values for transmit symbols from received signals with a given channel state information. The MMSE-PIC detection can be performed in an iterative manner, where the MMSE filtering and PIC are performed in parallel. Let $\hat{s}_t^{(u)}$ denote an estimate for a transmit symbol $s_t^{(u)}$, where a mean estimator is used. Consider a bitstream of length I representing a symbol $s_t^{(u)}$, where $I = \log_2 M$. We define $x_{t,i}^{(u)} = -1$ if the i-th bit of a bitstream representing $s_t^{(u)}$ is 1 and $x_{t,i}^{(u)} = 1$ otherwise. We also define a priori log-likelihood ratio (LLR) of $x_{t,i}^{(u)}$ as $L_a(x_{t,i}^{(u)}) = \log \frac{P(x_{t,i}^{(u)}=1)}{P(x_{t,i}^{(u)}=-1)}$ and define $\xi_{t,i}^{(u)} = \tanh\left(\frac{1}{2}L_a(x_{t,i}^{(u)})\right)$. Then, the estimate of $s_t^{(u)}$ is obtained by

$$\hat{s}_t^{(u)} = \sum_{a\in\mathcal{A}} aP\left\{s_t^{(u)} = a\right\} = \sum_{a\in\mathcal{A}} \frac{a}{2^I} \prod_{i=1}^{I}(1 + a_i\xi_{t,i}^{(u)}), \quad (2)$$

where $\mathcal{A}$ is a set of values for $s_t^{(u)}$ and a_i is the value of $x_{t,i}^{(u)}$ corresponding to $s_t^{(u)} = a$. We let $E_t^{(u)}$ denote the variance of $s_t^{(u)}$, which is obtained by

$$E_t^{(u)} = \sum_{a\in\mathcal{A}} \frac{|a|^2}{2^I} \prod_{i=1}^{I}(1 + a_i\xi_{t,i}^{(u)}) - \left|\hat{s}_t\right|^2. \quad (3)$$

The PIC process cancels all symbols other than a specific target symbol by using symbol estimates as

$$\hat{\mathbf{y}}_t^{(u)} = \mathbf{y}^{(u)} - \sum_{j=1,j\neq t}^{n_T} \mathbf{h}_j^{(u)}\hat{s}_j^{(u)} = \mathbf{h}_t^{(u)}s_t^{(u)} + \tilde{\mathbf{n}}_t^{(u)}, \quad (4)$$

where $\mathbf{h}_t^{(u)}$ is the t-th column of $\mathbf{H}^{(u)}$ and $\tilde{\mathbf{n}}_t^{(u)} \triangleq \sum_{j=1,j\neq t}^{n_T} \mathbf{h}_j^{(u)}e_j^{(u)} + \mathbf{n}^{(u)}$ with $e_j^{(u)} = s_j^{(u)} - \hat{s}_j^{(u)}$. The MMSE nulling matrix is obtained by

$$\begin{aligned}\mathbf{W}^{(u)H} &= \mathbf{H}^{(u)H}\left(\mathbf{H}^{(u)}\Delta^{(u)}\mathbf{H}^{(u)H} + \sigma^2\mathbf{I}\right)^{-1} \\ &= \left(\mathbf{H}^{(u)H}\mathbf{H}^{(u)}\Delta^{(u)} + \sigma^2\mathbf{I}\right)^{-1}\mathbf{H}^{(u)H}, \quad (5)\end{aligned}$$

where $\Delta^{(u)} = \text{diag}\left\{E_1^{(u)}, \cdots, E_{n_T}^{(u)}\right\}$. We apply a MMSE filter to $\hat{\mathbf{y}}_t^{(u)}$ and obtain $\hat{z}_t^{(u)} = \mathbf{w}_t^{(u)H}\hat{\mathbf{y}}_t^{(u)}$, where $\mathbf{w}_t^{(u)H}$ is the t-th row of $\mathbf{W}^{(u)H}$. Then, the MMSE filter output is expressed as

$$\hat{z}_t^{(u)} = \mathbf{w}_t^{(u)H}(\mathbf{h}_t^{(u)}s_t^{(u)} + \tilde{\mathbf{n}}_t^{(u)}) = \mu_t^{(u)}s_t^{(u)} + \mathbf{w}_t^{(u)H}\tilde{\mathbf{n}}_t^{(u)}, \quad (6)$$

where $\mu_t^{(u)} = \mathbf{w}_t^{(u)H}\mathbf{h}_t^{(u)}$. Note that for given $\mathbf{w}_t^{(u)}$ and $\mathbf{h}_t^{(u)}$, the random variable $\hat{z}_t^{(u)}$ is considered normally distributed with a mean $\mu_t^{(u)}s_t^{(u)}$ and a variance $\hat{\sigma}_t^{(u)2}$, where

$$\hat{\sigma}_t^{(u)2} = \mathbf{w}_t^{(u)H}E\left\{\tilde{\mathbf{n}}_t^{(u)}\tilde{\mathbf{n}}_t^{(u)H}\right\}\mathbf{w}_t^{(u)}. \quad (7)$$

Note that

$$E\left\{\tilde{\mathbf{n}}_t^{(u)}\tilde{\mathbf{n}}_t^{(u)H}\right\} = \sum_{j\neq t}\mathbf{h}_j^{(u)}E_j^{(u)}\mathbf{h}_j^{(u)H} + \sigma^2\mathbf{I}, \quad (8)$$

by using the independence between $e_j^{(u)}$ and $e_k^{(u)}$, $j \neq k$, and between $e_j^{(u)}$ and $n_k^{(u)}$, $\forall j, k$, with $E\{e_j^{(u)}\} = E\{n_j^{(u)}\} = 0$ and $E\{e_j^{(u)}e_j^{(u)*}\} = E_j^{(u)}$, $\forall j$. Then, (7) can be expanded as

$$\hat{\sigma}_t^{(u)2} = \mathbf{w}_t^{(u)H}\left(\mathbf{H}^{(u)}\Delta^{(u)}\mathbf{H}^{(u)H} + \sigma^2\mathbf{I}\right)\mathbf{w}_t^{(u)} - |\mu_t^{(u)}|^2E_t^{(u)}, \quad (9)$$

where $\mathbf{H}^{(u)}\Delta^{(u)}\mathbf{H}^{(u)H} = \sum_j \mathbf{h}_j^{(u)}E_j^{(u)}\mathbf{h}_j^{(u)H}$. By definition, $\mathbf{w}_t^{(u)H} = \mathbf{h}_t^{(u)H}(\mathbf{H}^{(u)}\Delta^{(u)}\mathbf{H}^{(u)H} + \sigma^2\mathbf{I})^{-1}$ so that (9) can be further expanded as

$$\hat{\sigma}_t^{(u)2} = \mathbf{w}_t^{(u)H}\mathbf{h}_t^{(u)} - |\mu_t^{(u)}|^2E_t^{(u)} = \mu_t^{(u)} - \mu_t^{(u)2}E_t^{(u)}. \quad (10)$$

We normalize MMSE filter output $\hat{z}_t^{(u)}$ as $z_t^{(u)} = \hat{z}_t^{(u)}/\mu_t^{(u)}$ whose distribution is Gaussian with a mean $s_t^{(u)}$ and a variance $1/\mu_t^{(u)} - E_t^{(u)}$. Then, the likelihood of $z_t^{(u)}$ for given $\mathbf{w}_t^{(u)}$ and $\mathbf{h}_t^{(u)}$ is determined as

$$p(z_t^{(u)}|s_t^{(u)} = a) = \frac{\rho_t^{(u)}}{\pi}\exp\left(-\rho_t^{(u)}|z_t^{(u)} - a|^2\right), \quad (11)$$

where $\rho_t^{(u)} = \frac{1}{2}\left((\mu_t^{(u)})^{-1} - E_t^{(u)}\right)^{-1}$. Let us define a posteriori LLR of $x_{t,i}^{(u)}$ as $L_d(x_{t,i}^{(u)}) = \log\frac{p(x_{t,i}^{(u)}=1|\mathbf{z}^{(u)})}{p(x_{t,i}^{(u)}=-1|\mathbf{z}^{(u)})}$, where $\mathbf{z}^{(u)} = \{z_1^{(u)}, \cdots, z_t^{(u)}, \cdots, z_{n_T}^{(u)}\}$. Then, we have

$$\begin{aligned} L_d(x_{t,i}^{(u)}) &= \log\frac{\sum_{a\in\mathcal{A}_i^{+1}}p(s_t^{(u)} = a|\mathbf{z}^{(u)})}{\sum_{a\in\mathcal{A}_i^{-1}}p(s_t^{(u)} = a|\mathbf{z}^{(u)})} \\ &= \log\frac{\sum_{a\in\mathcal{A}_i^{+1}}\prod_{m=1}^{n_T}p(z_m^{(u)}|s_t^{(u)} = a)p(a)}{\sum_{a\in\mathcal{A}_i^{-1}}\prod_{m=1}^{n_T}p(z_m^{(u)}|s_t^{(u)} = a)p(a)}, \end{aligned} \quad (12)$$

where $\mathcal{A}_i^{+1} = \{a|a_i = 1\}$ and $\mathcal{A}_i^{-1} = \{a|a_i = -1\}$. It is well known that the off-diagonal terms of $\mathbf{H}^{(u)H}\mathbf{H}^{(u)}$ become negligible compared to diagonal terms due to a channel hardening as the size of $\mathbf{H}^{(u)}$ grows [3]. Thus, $\mathbf{w}_t^{(u)H}$ has a dominant entry associated with $s_t^{(u)}$ and consequently, $z_t^{(u)} = s_t^{(u)} + \mathbf{w}_t^{(u)H}\tilde{\mathbf{n}}_t^{(u)}/\mathbf{w}_t^{(u)H}\mathbf{h}_t^{(u)}$ is dominated by $s_t^{(u)}$. It follows that $L_d(x_{t,i}^{(u)})$ is approximated as

$$L_d(x_{t,i}^{(u)}) \approx \log\frac{\sum_{a\in\mathcal{A}_i^{+1}}p(z_t^{(u)}|s_t^{(u)} = a)p(a)}{\sum_{a\in\mathcal{A}_i^{-1}}p(z_t^{(u)}|s_t^{(u)} = a)p(a)}. \quad (13)$$

Let us define an extrinsic LLR of $x_{t,i}^{(u)}$ as

$$L_e(x_{t,i}^{(u)}) = L_d(x_{t,i}^{(u)}) - L_a(x_{t,i}^{(u)}). \quad (14)$$

By using (11), (13), the property $P(x_{t,i}^{(u)} = a_i) = e^{a_iL_a(x_{t,i}^{(u)})/2}/(e^{L_a(x_{t,i}^{(u)})/2} + e^{-L_a(x_{t,i}^{(u)})/2})$ with $a_i = \pm 1$, and the approximation $\log\sum_i e^{-x_i} \approx -\min(x_i)$, we can approximate $L_e(x_{t,i}^{(u)})$ defined in (14) as

$$\begin{aligned} &L_e(x_{t,i}^{(u)}) \\ &\approx \log\frac{\sum_{a\in\mathcal{A}_i^{+1}}\exp\left(-\rho_t^{(u)}|z_t^{(u)} - a|^2 + \sum_{j=1,j\neq i}^{I}\frac{a_jL_a(x_{t,j}^{(u)})}{2}\right)}{\sum_{a\in\mathcal{A}_i^{-1}}\exp\left(-\rho_t^{(u)}|z_t^{(u)} - a|^2 + \sum_{j=1,j\neq i}^{I}\frac{a_jL_a(x_{t,j}^{(u)})}{2}\right)} \\ &\approx \min_{a\in\mathcal{A}_i^{-1}}\left\{\rho_t^{(u)}|z_t^{(u)} - a|^2 - \frac{1}{2}\sum_{j=1,j\neq i}^{I}a_jL_a(x_{t,j}^{(u)})\right\} \\ &\quad - \min_{a\in\mathcal{A}_i^{+1}}\left\{\rho_t^{(u)}|z_t^{(u)} - a|^2 - \frac{1}{2}\sum_{j=1,j\neq i}^{I}a_jL_a(x_{t,j}^{(u)})\right\}. \end{aligned} \quad (15)$$

The decision on the estimation for $x_{t,i}^{(u)}$ is made such that $x_{t,i}^{(u)} = 1$ if $L_d(x_{t,i}^{(u)}) \geq 0$ and $x_{t,i}^{(u)} = -1$ otherwise.

When MMSE-PIC detector is implemented in JDD process, a priori LLR $L_a(x_{t,i}^{(u)})$ is fed from the decoder and the extrinsic LLR $L_e(x_{t,i}^{(u)})$ generated in detector is delivered to the decoder. In most of conventional coded MIMO receivers, one detection iteration and one decoding iteration composes one global iteration. However, this mechanism needs to be modified to enhance the overall performance by allowing multiple detection iterations and decoding iterations in one global iteration. Inside local detection iterations, the sum of an extrinsic LLR $L_e(x_{t,i}^{(u)})$ obtained in the detector and a priori LLR $L_a(x_{t,i}^{(u)})$ fed from the decoder is used as a locally defined a priori LLR $L_a'(x_{t,i}^{(u)})$, i.e.,

$$L_a'(x_{t,i}^{(u)}) = L_a(x_{t,i}^{(u)}) + L_e(x_{t,i}^{(u)}). \quad (16)$$

In other words, $L_a'(x_{t,i}^{(u)})$ replaces $L_a(x_{t,i}^{(u)})$ in above equations used for message updates through detection iterations. Then, $L_a'(x_{t,i}^{(u)})$ is fed back to the detector and a new extrinsic LLR $L_e(x_{t,i}^{(u)})$ is obtained after performing processes introduced above. This procedure repeats for N_{det} detection iterations and the extrinsic LLR $L_e(x_{t,i}^{(u)})$ obtained at the final detection iteration is delivered to the decoder. Above operations related with adding LLR messages and setting direction of LLR message flows are the role of switch nodes placed at the output of detector. The detailed view of detection node is depicted in Fig. 3 and the MMSE-PIC algorithm is summarized in Algorithm 1.

Algorithm 1 MMSE-PIC Detection for Given u

1 Given $L_a(x_{t,i}^{(u)})$, initialize $L'_a(x_{t,i}^{(u)}) \leftarrow L_a(x_{t,i}^{(u)}), \forall t, i$
2 **for** $m = 1$ *to* N_{det} **do**
3 **for** $t = 1$ *to* n_T **do**
4 $\xi_{t,i}^{(u)} \leftarrow \tanh(\frac{1}{2}L'_a(x_{t,i}^{(u)})), \forall i$
5 $\hat{s}_t^{(u)} \leftarrow \sum_{a\in\mathcal{A}} \frac{a}{2^I} \prod_{i=1}^{I}(1 + a_i\xi_{t,i}^{(u)})$
6 $E_t^{(u)} = \sum_{a\in\mathcal{A}} \frac{|a|^2}{2^I} \prod_{i=1}^{I}(1 + a_i\xi_{t,i}^{(u)}) - |\hat{s}_i^{(u)}|^2$
7 $\Delta^{(u)} \leftarrow \text{diag}(E_1^{(u)}, E_2^{(u)}, \ldots, E_{n_T}^{(u)})$
8 $\mathbf{W}^{(u)H} \leftarrow \left(\mathbf{H}^{(u)H}\mathbf{H}^{(u)}\Delta^{(u)} + \sigma^2\mathbf{I}\right)^{-1}\mathbf{H}^{(u)H}$
9 **for** $t = 1$ *to* n_T **do**
10 $\mu_t^{(u)} \leftarrow \mathbf{w}_t^{(u)H}\mathbf{h}_t^{(u)}$
11 $\rho_t^{(u)} \leftarrow ((\mu_t^{(u)})^{-1} - E_t^{(u)})^{-1}/2$
12 $\hat{\mathbf{y}}_t^{(u)} \leftarrow \mathbf{y}^{(u)} - \sum_{j=1,j\neq t}^{n_T} \mathbf{h}_j^{(u)}\hat{s}_j^{(u)}$
13 $z_t^{(u)} \leftarrow \mathbf{w}_t^{(u)H}\hat{\mathbf{y}}_t^{(u)}/\mu_t^{(u)}$
14 $L_e(x_{t,i}^{(u)}) \leftarrow \min_{a\in\mathcal{A}_i^{-1}} \{\rho_t^{(u)}|z_t^{(u)} - a|^2 - \frac{1}{2}\sum_{j\neq i} a_j L'_a(x_{t,j}^{(u)})\} - \min_{a\in\mathcal{A}_i^{+1}} \{\rho_t^{(u)}|z_t^{(u)} - a|^2 - \frac{1}{2}\sum_{j\neq i} a_j L'_a(x_{t,j}^{(u)})\}, \forall i$
15 $L'_a(x_{t,i}^{(u)}) \leftarrow L_a(x_{t,i}^{(u)}) + L_e(x_{t,i}^{(u)}), \forall i$

Algorithm 2 Approximate MMSE-PIC Detection for Given u

1 Given $L_a(x_{t,i}^{(u)})$, initialize $L'_a(x_{t,i}^{(u)}) \leftarrow L_a(x_{t,i}^{(u)}), \forall t, i$
2 **for** $m = 1$ *to* N_{det} **do**
3 **for** $t = 1$ *to* n_T **do**
4 $\xi_{t,i}^{(u)} \leftarrow \tanh(\frac{1}{2}L'_a(x_{t,i}^{(u)})), \forall i$
5 $\hat{s}_t^{(u)} \leftarrow \sum_{a\in\mathcal{A}} \frac{a}{2^I} \prod_{i=1}^{I}(1 + a_i\xi_{t,i}^{(u)})$
6 $E_t^{(u)} = \sum_{a\in\mathcal{A}} \frac{|a|^2}{2^I} \prod_{i=1}^{I}(1 + a_i\xi_{t,i}^{(u)}) - |\hat{s}_i^{(u)}|^2$
7 $\mathbf{w}_t^{(u)H} \leftarrow \mathbf{h}_t^{(u)H}/(||\mathbf{h}_t^{(u)}||^2E_t^{(u)} + \sigma^2)$
8 $\mu_t^{(u)} \leftarrow \mathbf{w}_t^{(u)H}\mathbf{h}_t^{(u)}$
9 $\rho_t^{(u)} \leftarrow ((\mu_t^{(u)})^{-1} - E_t^{(u)})^{-1}/2$
10 **for** $t = 1$ *to* n_T **do**
11 $\hat{\mathbf{y}}_t^{(u)} \leftarrow \mathbf{y}^{(u)} - \sum_{j=1,j\neq t}^{n_T} \mathbf{h}_j^{(u)}\hat{s}_j^{(u)}$
12 $z_t^{(u)} \leftarrow \mathbf{w}_t^{(u)H}\hat{\mathbf{y}}_t^{(u)}/\mu_t^{(u)}$
13 $L_e(x_{t,i}^{(u)}) \leftarrow \min_{a\in\mathcal{A}_i^{-1}} \{\rho_t^{(u)}|z_t^{(u)} - a|^2 - \frac{1}{2}\sum_{j\neq i} a_j L'_a(x_{t,j}^{(u)})\} - \min_{a\in\mathcal{A}_i^{+1}} \{\rho_t^{(u)}|z_t^{(u)} - a|^2 - \frac{1}{2}\sum_{j\neq i} a_j L'_a(x_{t,j}^{(u)})\}, \forall i$
14 $L'_a(x_{t,i}^{(u)}) \leftarrow L_a(x_{t,i}^{(u)}) + L_e(x_{t,i}^{(u)}), \forall i$

2) APPROXIMATE MMSE-PIC DETECTION

As mentioned earlier, the off-diagonal terms of $\mathbf{H}^{(u)H}\mathbf{H}^{(u)}$ become smaller compared to diagonal terms due to a channel hardening as the size of $\mathbf{H}^{(u)}$ grows [3]. It follows that $\mathbf{H}^{(u)H}\mathbf{H}^{(u)}\Delta + \sigma^2\mathbf{I}$ can be approximated by a diagonal matrix as

$$\mathbf{H}^{(u)H}\mathbf{H}^{(u)}\Delta + \sigma^2\mathbf{I} \approx \begin{bmatrix} \tilde{w}_{1,1}^{(u)} & 0 & \cdots & 0 \\ 0 & \tilde{w}_{2,2}^{(u)} & \cdots & 0 \\ \vdots & \vdots & \ddots & 0 \\ 0 & 0 & \cdots & \tilde{w}_{n_T,n_T}^{(u)} \end{bmatrix}, \tag{17}$$

where

$$\tilde{w}_{t,t}^{(u)} = ||\mathbf{h}_t^{(u)}||^2E_t^{(u)} + \sigma^2 = \sum_{j=1}^{n_R} |h_{j,t}^{(u)}|^2E_t^{(u)} + \sigma^2, \tag{18}$$

$t = 1, \cdots, n_T$. Then, the MMSE nulling matrix defined in (5) can be approximated as

$$\begin{aligned}\mathbf{W}^{(u)H} &= \left(\mathbf{H}^{(u)H}\mathbf{H}^{(u)}\Delta + \sigma^2\mathbf{I}\right)^{-1}\mathbf{H}^{(u)H} \\ &\approx \begin{bmatrix} \frac{1}{\tilde{w}_{1,1}^{(u)}} & 0 & \cdots & 0 \\ 0 & \frac{1}{\tilde{w}_{2,2}^{(u)}} & \cdots & 0 \\ \vdots & \vdots & \cdots & 0 \\ 0 & 0 & \cdots & \frac{1}{\tilde{w}_{n_T,n_T}^{(u)}} \end{bmatrix} \begin{bmatrix} \mathbf{h}_1^{(u)H} \\ \mathbf{h}_2^{(u)H} \\ \vdots \\ \mathbf{h}_{n_T}^{(u)H} \end{bmatrix},\end{aligned} \tag{19}$$

whose t-th row is expressed by

$$\mathbf{w}_t^{(u)H} \approx \frac{1}{\tilde{w}_{t,t}^{(u)}}\mathbf{h}_t^{(u)H} = \frac{\mathbf{h}_t^{(u)H}}{||\mathbf{h}_t^{(u)}||^2E_t^{(u)} + \sigma^2}. \tag{20}$$

Consequently, (20) replaces Line 8 in Algorithm 1 and the resultant Approximate MMSE-PIC is summarized in Algorithm 2.

3) GAUSS-SEIDEL-AIDED MMSE-PIC DETECTION

To relieve high computational complexity incurred by a matrix inversion used to compute MMSE nulling matrix, we apply a Gauss-Seidel algorithm which is able to find a solution of a matrix equation in an iterative manner. Let

$$\hat{\mathbf{z}}^{(u)} = \mathbf{W}^{(u)H}\hat{\mathbf{y}}_t^{(u)}, \tag{21}$$

where $\hat{\mathbf{z}}^{(u)} = [\hat{z}_1^{(u)}, \hat{z}_2^{(u)}, \cdots, \hat{z}_t^{(u)}]^T$. We reformulate (21) by multiplying $\mathbf{G}^{(u)} = \mathbf{H}^{(u)H}\mathbf{H}^{(u)}\Delta + \sigma^2\mathbf{I}$ to the left of both sides as

$$\mathbf{G}^{(u)}\hat{\mathbf{z}}^{(u)} = \mathbf{G}^{(u)}\mathbf{W}^{(u)H}\hat{\mathbf{y}}_t^{(u)} = \mathbf{H}^{(u)H}\hat{\mathbf{y}}_t^{(u)}. \tag{22}$$

By applying Gauss-Seidel algorithm, we solve (21) via (22) in an iterative manner, where entries of $\hat{\mathbf{z}}^{(u)}$ are recursively updated. The t-th entry of $\hat{\mathbf{z}}^{(u)}$ obtained at the ℓ-th iteration of Gauss-Seidel algorithm is denoted by $\tilde{z}_t^{(u)}[\ell]$ and obtained by [20]

$$\begin{aligned}\tilde{z}_t^{(u)}[\ell] = \frac{1}{g_{t,t}^{(u)}}\Bigg(&\mathbf{h}_t^{(u)H}\hat{\mathbf{y}}_t^{(u)} - \sum_{j<t} g_{t,j}^{(u)}\tilde{z}_j^{(u)}[\ell] \\ &- \sum_{j>t} g_{t,j}^{(u)}\tilde{z}_j^{(u)}[\ell-1]\Bigg),\end{aligned} \tag{23}$$

where $g_{i,j}^{(u)}$ denotes the (i,j)-th entry of $\mathbf{G}^{(u)}$. The initial value $\tilde{z}_t^{(u)}[0]$ is determined from (22) by using the diagonal

Algorithm 3 Gauss-Seidel-Aided MMSE-PIC Detection for Given u

Given $L_a(x_{t,i}^{(u)})$, initialize $L'_a(x_{t,i}^{(u)}) \leftarrow L_a(x_{t,i}^{(u)})$, $\forall t, i$
for $m = 1$ *to* N_{det} **do**
  for $t = 1$ *to* n_T **do**
    $\xi_{t,i}^{(u)} \leftarrow \tanh(\frac{1}{2}L'_a(x_{t,i}^{(u)}))$, $\forall i$
    $\hat{s}_t^{(u)} \leftarrow \sum_{a\in\mathcal{A}} \frac{a}{2^I} \prod_{i=1}^{I}(1 + a_i\xi_{t,i}^{(u)})$
    $E_t^{(u)} = \sum_{a\in\mathcal{A}} \frac{|a|^2}{2^I} \prod_{i=1}^{I}(1 + a_i\xi_{t,i}^{(u)}) - |\hat{s}_i^{(u)}|^2$
    $g_{t,t}^{(u)} \leftarrow ||\mathbf{h}_t^{(u)}||^2 E_t^{(u)} + \sigma^2$
    $\mu_t^{(u)} \leftarrow ||\mathbf{h}_t^{(u)}||^2 / g_{t,t}^{(u)}$
    $\rho_t^{(u)} \leftarrow ((\mu_t^{(u)})^{-1} - E_t^{(u)})^{-1}/2$
  for $t = 1$ *to* n_T **do**
    $\hat{\mathbf{y}}_t^{(u)} \leftarrow \mathbf{y}^{(u)} - \sum_{j=1, j\neq t}^{n_T} \mathbf{h}_j^{(u)} \hat{s}_j^{(u)}$
    $\tilde{z}_t^{(u)}[0] \leftarrow \frac{1}{g_{t,t}^{(u)}} \mathbf{h}_t^{(u)H} \hat{\mathbf{y}}_t^{(u)}$
    for $\ell = 1$ *to* n_{GS} **do**
      $\tilde{z}_t^{(u)}[\ell] \leftarrow \tilde{z}_t^{(u)}[0] - \frac{1}{g_{t,t}^{(u)}} \big(\sum_{j<t} g_{t,j}^{(u)} \tilde{z}_j^{(u)}[\ell] + \sum_{j>t} g_{t,j}^{(u)} \tilde{z}_j^{(u)}[\ell - 1] \big)$
    $z_t^{(u)} \leftarrow \tilde{z}_t^{(u)}[\ell] / \mu_t^{(u)}$
    $L_e(x_{t,i}^{(u)}) \leftarrow \min_{a\in\mathcal{A}_i^{-1}} \{\rho_t^{(u)} |z_t^{(u)} - a|^2 - \frac{1}{2}\sum_{j\neq i} a_j L'_a(x_{t,j}^{(u)})\} - \min_{a\in\mathcal{A}_i^{+1}} \{\rho_t^{(u)} |z_t^{(u)} - a|^2 - \frac{1}{2}\sum_{j\neq i} a_j L'_a(x_{t,j}^{(u)})\}$, $\forall i$
    $L'_a(x_{t,i}^{(u)}) \leftarrow L_a(x_{t,i}^{(u)}) + L_e(x_{t,i}^{(u)})$, $\forall i$

approximation for $\mathbf{G}^{(u)}$ as

$$\tilde{z}_t^{(u)}[0] = \frac{1}{g_{t,t}^{(u)}} \mathbf{h}_t^{(u)H} \hat{\mathbf{y}}_t^{(u)}, \tag{24}$$

where $g_{t,t}^{(u)} = ||\mathbf{h}_t^{(u)}||^2 E_t^{(u)} + \sigma^2$. We also apply a diagonal approximation for $\mathbf{G}^{(u)}$ to determine $\mu_t^{(u)}$. Since $\mathbf{W}^{(u)H} = (\mathbf{G}^{(u)})^{-1}\mathbf{H}^{(u)H}$ and $(\mathbf{G}^{(u)})^{-1} \approx \text{diag}\{1/g_{1,1}^{(u)}, \cdots, 1/g_{n_T,n_T}^{(u)}\}$, we obtain an approximation $\mathbf{w}_t^{(u)H} = \mathbf{h}_t^{(u)H}/g_{t,t}^{(u)}$, and consequently

$$\mu_t^{(u)} = \mathbf{w}_t^{(u)H} \mathbf{h}_t^{(u)} = \frac{1}{g_{t,t}^{(u)}} ||\mathbf{h}_t^{(u)}||^2. \tag{25}$$

The Gauss-Seidel-aided MMSE-PIC detection is summarized in Algorithm 3. Note that the Gauss-Seidel iteration is included as a subloop in the detection iteration, where n_{GS} denotes the number of Gauss-Seidel iterations performed in each detection iteration.

B. DECODING

Each LDPC decoder is represented by a bitartite factor graph composed of N variable nodes and $N - K$ check nodes connected by edges as shown in Fig. 2. Given channel LLRs fed to variable nodes, soft LLR messages regarding code bits are computed at all variable nodes and check nodes in an iterative manner with messages exchanged between two classes of nodes. Let L_v denote the channel LLR available at the variable node v, L_{vc} denote the message sent from the variable node v to the check node c, and L_{cv} denote the message sent from the check node c to the variable node v. Then, LLR messages are updated by a sum-product algorithm [26], [30] as

$$L_{vc} = L_v + \sum_{c'\in C_v\backslash c} L_{c'v} \tag{26}$$

in variable nodes and

$$L_{cv} = \prod_{v'\in V_c\backslash v} \text{sign}(L_{v'c}) \cdot \phi\Big(\sum_{v'\in V_c\backslash v} \phi\left(|L_{v'c}|\right) \Big) \tag{27}$$

in check nodes, where $\phi(x) = \log\frac{\exp(x)+1}{\exp(x)-1}$. Note that $C_v\backslash c$ denotes the set of check nodes except c connected to the variable node v and $V_c\backslash v$ denotes the set of variable nodes except v connected to the check node c. The message updates and message exchange between nodes introduced above describes local iterations of decoding. Thus, one local decoding iteration consists of a sequence of variable node update, message delivery from variable node to check node, check node update and message delivery from check node to variable node.

Let us consider message exchange between detectors and decoders. As depicted in Fig. 2, the u-th group of $\log_2 M$ variable nodes in each decoder are connected to the u-th detection node via switch nodes. We focus on the t-th decoder and let $p = i + (u-1)\cdot\log_2 M$, $1 \le i \le \log_2 M$. The extrinsic LLR $L_e(x_{t,i}^{(u)})$ obtained in the u-th detection node is delivered to the p-th variable node in the t-th decoder, denoted by v_p^t. Then, $L_e(x_{t,i}^{(u)})$ is used as the channel LLR at the variable node $v = v_p^t$, i.e., $L_v = L_e(x_{t,i}^{(u)})$ in (26), and decoding iterations proceed.

After N_{dec} decoding iterations, each variable node sums up all LLR messages sent from connected check nodes and delivers the summed result to the detection node, which is used as a priori LLR in the detector at the next global iteration. In other words, $L_a(x_{t,i}^{(u)})$ sent to the detector as a priori LLR is obtained by

$$L_a(x_{t,i}^{(u)}) = \sum_{c\in C_{v_p^t}} L_{cv_p^t}, \tag{28}$$

where $L_{cv_p^t}$ is obtained at the N_{dec}-th decoding iteration. After N_g global iterations, we make decision on each code bit as the following. The code bit is decoded as 0 if $L_a(x_{t,i}^{(u)}) \ge 0$, and 1 otherwise. The overall JDD process is summarized in Algorithm 4.

IV. EXIT ANALYSIS FOR THE BEHAVIOR OF JOINT DETECTION AND DECODING

Behavior of iterative JDD processes can be investigated by using the EXIT analysis [31]. Under the assumption that LLR messages in the same stage are i.i.d., we propose an EXIT analysis tool for analyzing the behavior of JDD process of

Algorithm 4 Joint Detection and Decoding (JDD) Algorithm

Initialize $L_a(x_{t,i}^{(u)}) \leftarrow 0, \forall u, t, i$ and $L_{cv} \leftarrow 0, \forall v, c$
for $l = 1$ *to* N_g **do**
  for $u = 1$ *to* U **do**
    for $m = 1$ *to* N_{det} **do**
      Run Detection Algorithm for the u-th detector
    Compute $L_e(x_{t,i}^{(u)}), \forall t, i$ by (15)
  for $t = 1$ *to* N_t **do**
    $v \leftarrow i + (u-1)\log_2 M, \forall u, i$
    $L_v \leftarrow L_e(x_{t,i}^{(u)})$
    for $l' = 1$ *to* N_{dec} **do**
      Update $L_{vc}, \forall v$ by (26)
      Update $L_{cv}, \forall c$ by (27)
    Update $L_a(x_{t,i}^{(u)}), \forall u, i$ by (28)
Decide each code bit based on the sign of $L_a(x_{t,i}^{(u)})$, $\forall u, t, i$

coded massive MIMO system. We focus on the bit-level EXIT characteristics of all component units in the JDD process in the receiver. Let I_A denote a mutual information between a code bit, or equivalently a binary symbol $x_{t,i}^{(u)}$, and the corresponding a priori LLR message $L'_a(x_{t,i}^{(u)})$ of detector. We also let I_E be a mutual information between a code bit and the corresponding extrinsic LLR message $L_e(x_{t,i}^{(u)})$ of detector. Then, we regard the detector as an EXIT module generating I_E for a given input I_A, where a channel SNR is used as a parameter. We let I_{CV} be a mutual information between a code bit and the LLR message L_{cv} while we let I_{VC} be a mutual information between a code bit and a LLR message L_{vc}. Then, the message update at variable node in decoder can be interpreted as an EXIT function generating I_{VC} for a given input I_{CV} with a parameter I_E. The message update at check node is considered an EXIT function generating I_{CV} for a given input I_{VC}.

Allowing a slight abuse of notation, we express I_{CV} associated with degree-d_c check nodes as $I_{CV}(d_c)$ and I_{VC} associated with degree-d_v variable nodes as $I_{VC}(d_v)$. In a similar manner, we use $I_A(d_v)$ and $I_E(d_v)$ to denote I_A and I_E, respectively, that are associated with degree-d_v variable nodes. Then, we define average mutual information over all degrees as $\bar{I}_{CV} = \sum_{d_c=2}^{d_{c,\max}} \rho_{d_c} I_{CV}(d_c)$ and $\bar{I}_{VC} = \sum_{d_v=2}^{d_{v,\max}} \lambda_{d_v} I_{VC}(d_v)$, where λ_{d_v} and ρ_{d_c} denote the fractions of edges that are connected to degree-d_v variable nodes and degree-d_c check nodes, respectively, and $d_{v,\max}$ and $d_{c,\max}$ are maxima of d_v and d_c, respectively.

Under the assumption of normal distribution of LLR message, the mutual information between a code bit and a LLR message can be expressed by a function of variance or standard deviation as [32]

$$J(\sigma_L) = 1 - \int_{-\infty}^{\infty} \frac{e^{-(\xi-\sigma_L^2/2)^2/2\sigma_L^2}}{\sqrt{2\pi\sigma_L^2}} \cdot \log_2[1+e^{-\xi}]d\xi, \tag{29}$$

where σ_L^2 is the variance of a normally distributed LLR message L. Since a locally defined a priori LLR message of detector is obtained by (16) and (28), we can obtain $I_A(d_v)$ by

$$I_A(d_v) = J\left(\sqrt{[J^{-1}(I_E(d_v))]^2 + d_v \cdot [J^{-1}(\bar{I}_{CV})]^2}\right). \tag{30}$$

Note that $I_E(d_v)$ is defined as a function of $I_A(d_v)$ with a parameter of channel SNR, i.e.,

$$I_E(d_v) = f_O\left(I_A(d_v), \frac{E_b}{N_0}\right), \tag{31}$$

where $f_O()$ is expressed in a polynomial form, and it is obtained by Monte Carlo simulation and a curve fitting technique. At variable nodes, the message going to a target check node is generated by summing up all incoming messages except one from a target check node, so L_{vc} is obtained by summing up the extrinsic LLR message of detector and $(d_v - 1)$ copies of L_{cv}. Then, $I_{VC}(d_v)$ is obtained as

$$I_{VC}(d_v) = J\left(\sqrt{\left[J^{-1}\left(I_E(d_v)\right)\right]^2 + (d_v-1)\cdot\left[J^{-1}\left(\bar{I}_{CV}\right)\right]^2}\right), \tag{32}$$

where the EXIT function of check node is approximated by [32]

$$I_{CV}(d_c) \approx 1 - J\left(\sqrt{d_c - 1} \cdot J^{-1}(1 - \bar{I}_{VC})\right). \tag{33}$$

The density evolution of soft messages in the JDD process in terms of EXIT characteristics is summarized in Algorithm 5. By running Algorithm 5, the update of average mutual information $\bar{I}_{VC}$ over iterations can be traced. If the value of $\bar{I}_{VC}$ reaches 1 after iterations at a certain E_b/N_0, the JDD process is interpreted to converge and the decoding succeeds at this E_b/N_0. The lowest value of E_b/N_0 at which JDD converges is defined as a threshold. In case that an iterative process can be described by a 2-D EXIT chart consisting of two EXIT curves, it is easy to predict whether or not the mutual information reaches 1 and decoding succeeds. If a tunnel is observed between two EXIT curves, a decoding trajectory penetrates the tunnel and reaches the highest value of mutual information, which implies a successful decoding. However, if a higher dimensional EXIT chart is defined as in a coded massive MIMO system, detecting a tunnel by a visual inspection is not easy any more. Thus, we need to trace the value of $\bar{I}_{VC}$ by running Algorithm 5 to judge the convergence of JDD process.

Let us consider 3-D EXIT chart of JDD for coded massive MIMO system obtained as a by-product of running Algorithm 5. A 3-D EXIT chart is composed of two EXIT surfaces, each of which represents EXIT characteristics

Algorithm 5 EXIT Analysis for JDD Process

Initialize: $\bar{I}_{CV} \leftarrow 0$ and $I_E(d_v) \leftarrow 0, \forall d_v$
for $l = 1$ *to* N_g **do**
  for $d_v = 2$ *to* $d_{v,\max}$ **do**
    for $l' = 1$ *to* N_{det} **do**
      $I_E(d_v) \leftarrow f_O\left(J\left(\sqrt{[J^{-1}(I_E(d_v))]^2 + d_v \cdot [J^{-1}(\bar{I}_{CV})]^2}\right), \frac{E_b}{N_0}\right)$
  $\bar{I}_E \leftarrow \sum_{d_v=2}^{d_{v,\max}} \lambda_{d_v} I_E(d_v)$
  for $l'' = 1$ *to* N_{dec} **do**
    $\bar{I}_{VC} \leftarrow \sum_{d_v=2}^{d_{v,\max}} \lambda_{d_v} \cdot J\left(\sqrt{\left[J^{-1}\left(I_E(d_v)\right)\right]^2 + (d_v - 1)\cdot\left[J^{-1}\left(\bar{I}_{CV}\right)\right]^2}\right)$
    $\bar{I}_{CV} \leftarrow \sum_{d_c=2}^{d_{c,\max}} \rho_{d_c}\cdot\left(1 - J\left(\sqrt{d_c - 1}\cdot J^{-1}(1 - \bar{I}_{VC})\right)\right)$

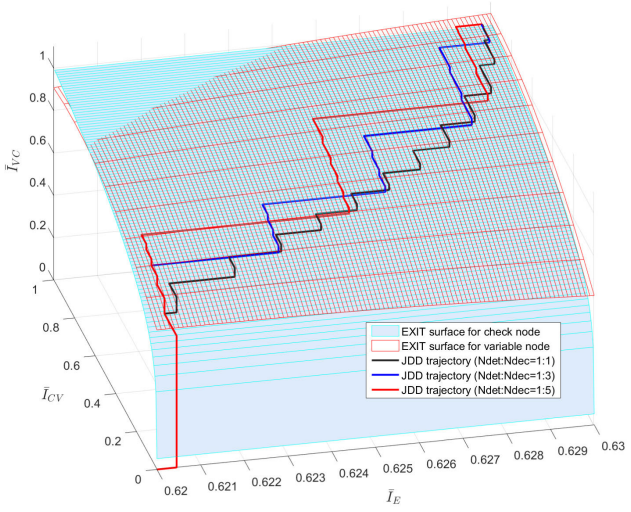

FIGURE 4. 3-D EXIT chart and trajectory of JDD for (3, 6)-regular LDPC coded multi-user massive MIMO system with $n_T = 4$ and $n_R = 16$ at $E_b/N_0 = -7$[dB], where QPSK is used for modulation. Note that $\bar{I}_E$ denotes the mutual information per observation node.

of variable node and check node, respectively. The space between two EXIT surfaces may or may not form an unblocked tunnel from the entry to the exit. If an unblocked tunnel is formed, the JDD trajectory will travel through the tunnel by a 3D zigzag movement to reach the point of $\bar{I}_{VC} = 1$. In this case, the JDD process converges and a low BER can be obtained. On the other hand, if the space between two EXIT surfaces does not form an unblocked tunnel, the JDD trajectory will get stuck at a certain point of $\bar{I}_{VC} < 1$, resulting in a high BER. The JDD trajectory can be obtained by connecting the points of $\bar{I}_{VC}$, $\bar{I}_{CV}$, and $\bar{I}_E$ obtained by running Algorithm 5 with straight lines. The trajectory moves straight in the direction of $\bar{I}_E$-axis by a detection iteration and experiences a pair of orthogonal movements on the $\bar{I}_{VC}$-$\bar{I}_{CV}$ plane by a decoding iteration. In Fig. 4, we plot several JDD trajectories obtained by using distinct JDD strategies, which are defined as the ratio of $N_{det} : N_{dec}$ composing a global iteration. It is observed that different JDD strategies result in different JDD trajectories. The JDD trajectory reaching $\bar{I}_{VC} = 1$ with a small number of zigzag movements implies fast convergence of JDD process. Since a tunnel formed between two EXIT surfaces is uneven, an efficient strategy for trajectory movement should be designed to obtain the fast convergence of JDD process. We achieve this goal by choosing appropriate JDD strategy for a given detection algorithm and accordingly designing LDPC codes.

V. OPTIMAL DESIGN OF LDPC CODES AND JDD STRATEGY

In building LDPC coded multi-user massive MIMO systems, there exist two main design parameters: the degree distribution of LDPC codes and the JDD strategy meaning the ratio of $N_{det} : N_{dec}$ composing one global iteration. The first design parameter determines the threshold and the second design parameter determines the convergence speed of JDD. Our design goal is a strong error correcting capability resulting in a low BER and a fast convergence speed of JDD algorithm. For this purpose, we utilize the EXIT analysis tool proposed in Sec. IV. To evaluate the convergence speed, we trace the evolution of $\bar{I}_{VC}$ with respect to the total number of local iterations by running Algorithm 5 as shown in Fig. 5 - Fig. 10. Recall that a local iteration means each detection iteration and decoding iteration. Note that running N_g global iterations with the ratio $N_{det} : N_{dec}$ results in $N_g(N_{det} + N_{dec})$ local iterations when MMSE-PIC and Approximate MMSE-PIC detection schemes are employed. When Gauss-Seidel-aided MMSE-PIC detection scheme is used, the total number of local iterations becomes $N_g(N_{det}n_{GS} + N_{dec})$.

LDPC codes are designed via degree distribution optimization followed by edge placement between variable nodes and check nodes. We determine $\boldsymbol{\lambda} = \{\lambda_2, \cdots, \lambda_{d_{v,max}}\}$ and $\boldsymbol{\rho} = \{\rho_2, \cdots, \rho_{d_{c,max}}\}$ to maximize the code rate $R(\boldsymbol{\lambda}, \boldsymbol{\rho})$ with convergence of JDD guaranteed at a given E_b/N_0 by using EXIT analysis, where the code rate is defined by [26]

$$R(\boldsymbol{\lambda}, \boldsymbol{\rho}) = 1 - \frac{\sum_{d_c=2}^{d_{c,\max}} \rho_{d_c}/d_c}{\sum_{d_v=2}^{d_{v,\max}} \lambda_{d_v}/d_v}. \tag{34}$$

For a given target code rate, we run Algorithm 5 for various E_b/N_0 and find the smallest E_b/N_0 resulting in the maximum $R(\boldsymbol{\lambda}, \boldsymbol{\rho})$ exceeding the target code rate. Such E_b/N_0 is defined as the threshold and it is denoted by $(E_b/N_0)^*$. The corresponding degree distributions are considered optimal and denoted by $(\boldsymbol{\lambda}^*, \boldsymbol{\rho}^*)$.

Next, we place edges between variable nodes and check nodes based on $(\boldsymbol{\lambda}^*, \boldsymbol{\rho}^*)$ to satisfy the following criteria [26]:

(a) Short cycles involving only degree-2 variable nodes should be avoided.
(b) Length-4 cycles should be avoided.
(c) All degree-2 variable nodes should represent only non-systematic bits.

The criteria (a) and (b) can be satisfied by applying the progressive edge growth (PEG) algorithm [49], and the criterion (c) can be satisfied by a condition

$$\lambda_2 \leq 2 \sum_{d_c=2}^{d_{c,\max}} \rho_{d_c}/d_c, \tag{35}$$

which can be incorporated in the degree distribution optimization process as a constraint [36]. Then, the degree distribution for a given E_b/N_0 is determined as

$$\begin{aligned} &\max_{\boldsymbol{\lambda},\boldsymbol{\rho}} \quad R(\boldsymbol{\lambda}, \boldsymbol{\rho}) \\ &\text{s.t.} \quad \bar{I}_{VC} = 1 \text{ as a result of running Algorithm 5,} \\ &\qquad \lambda_2 \leq 2 \sum_{d_c=2}^{d_{c,\max}} \rho_{d_c}/d_c, \\ &\qquad \sum_{d_c=2}^{d_{c,\max}} \rho_{d_c} = \sum_{d_v=2}^{d_{v,\max}} \lambda_{d_v} = 1 \quad \text{with} \quad \rho_{d_c}, \lambda_{d_v} \geq 0, \end{aligned} \tag{36}$$

where the first constraint ensures the convergence of JDD and the second constraint satisfies the criterion (c).

We also need to consider the convergence speed of JDD algorithm when designing LDPC codes. The convergence speed is determined by the harmony of degree distribution and JDD strategy. We predict the convergence speed of JDD by observing the evolution of $\bar{I}_{VC}$ with respect to the number of local iterations as shown in Fig. 5 - Fig. 10. The degree distribution achieving $(E_b/N_0)^*$ as well as the fastest JDD convergence will be considered the overall optimal and will be denoted as $(\boldsymbol{\lambda}^\dagger, \boldsymbol{\rho}^\dagger)$.

In summary, LDPC codes and JDD strategy for multi-user massive MIMO system are designed by the following procedure:

(i) Perform the degree distribution optimization (36) for various E_b/N_0 and candidate JDD strategies.
(ii) Determine $(E_b/N_0)^*$ and the optimal JDD strategy, and find the corresponding degree distribution $(\boldsymbol{\lambda}^\dagger, \boldsymbol{\rho}^\dagger)$.
(iii) Construct the parity-check matrix of LDPC codes from $(\boldsymbol{\lambda}^\dagger, \boldsymbol{\rho}^\dagger)$ by using the PEG algorithm.

By following the above procedure, we can efficiently construct LDPC codes and JDD mechanism for multi-user massive MIMO system showing a lower threshold $(E_b/N_0)^*$, or equivalently a better error correcting capability, and a faster convergence of JDD.

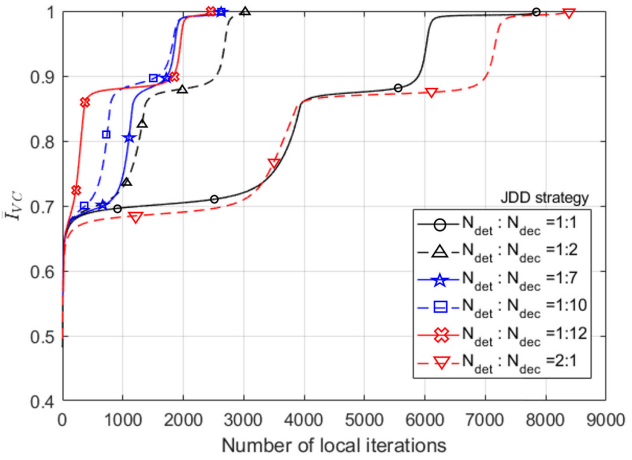

FIGURE 5. Evolution of $\bar{I}_{VC}$ with respect to the number of local iterations for some JDD strategies with MMSE-PIC detection, where $R = 1/2$, $n_T = 4$, $n_R = 16$.

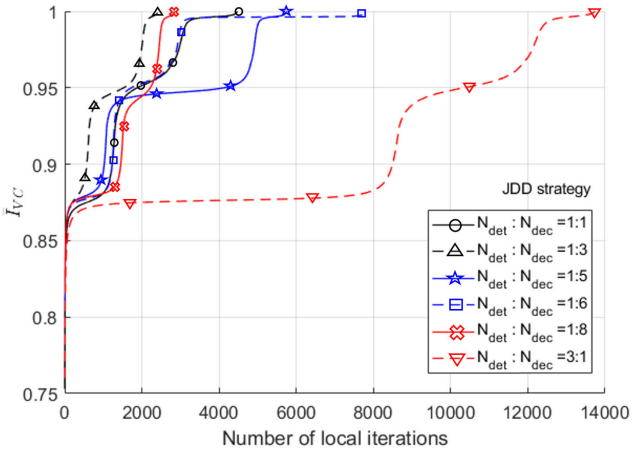

FIGURE 6. Evolution of $\bar{I}_{VC}$ with respect to the number of local iterations for some JDD strategies with MMSE-PIC detection, where $R = 3/4$, $n_T = 4$, $n_R = 64$.

VI. NUMERICAL RESULTS

We consider LDPC coded multi-user massive MIMO systems with 4 UEs and 16 or 64 receive antennas at BS, i.e., $n_T = 4$ and $n_R = 16$ or 64. We regard the multi-user massive MIMO system with n_T UEs and n_R BS antennas as $n_T \times n_R$ channel. Each UE encodes information bits to rate-1/2 or 3/4 LDPC codes and maps code bits to QPSK symbols by Gray-mapping. The channel gain of each pair of UE and BS antenna is characterized as an i.i.d. complex Gaussian random variable with zero mean and unit variance. The additive noise at BS antenna is supposed to be i.i.d. zero-mean circular symmetric complex white Gaussian noise. We consider an iterative JDD process at the receiver which employs MMSE-PIC, Approximate MMSE-PIC and Gauss-Seidel-aided MMSE-PIC as a detection algorithm, where the

TABLE 1. Optimal degree distributions (λ^*, ρ^*) of rate-1/2 LDPC codes for multi-user massive MIMO system with MMSE-PIC for some candidate JDD strategies, where $(n_T \times n_R) = (4 \times 16)$ and (4×64) are considered, and $d_{v,\max} = 24$ is used.

$n_T \times n_R$	4×16						4×64					
$N_{det} : N_{dec}$	$1:1$	$1:2$	$1:7$	**$1:10$**	$1:12$	$2:1$	$1:1$	$1:2$	**$1:5$**	$1:9$	$1:14$	$4:1$
λ_2	0.25363	0.2498	0.25261	**0.25059**	0.2515	0.25301	0.24819	0.24773	**0.24526**	0.24639	0.24787	0.24754
λ_3	0.1544	0.19239	0.19546	**0.21222**	0.19157	0.16423	0.193	0.19917	**0.21218**	0.22004	0.20148	0.2098
λ_4	0.10642	0.03324	0.00945	**0.00597**	0.01326	0.01552	0.00886	0.05319	**0.00138**	0.00138	0.00908	0.0138
λ_5	0.04595	0.07836	0.1058	**0.02986**	0.10397	0.20863	0.12257	0.0087	**0.07014**	0.00055	0.06829	0.00976
λ_6												
λ_7	0.0542	0.05088	0.0545	**0.18012**	0.11525		0.09573	0.04557	**0.1497**	0.2709	0.14223	0.27812
λ_8	0.08812	0.12087	0.09674	**0.08412**	0.03574			0.23181	**0.04698**	0.04617	0.09661	0.01514
λ_9						0.05197	0.04927					
λ_{10}	0.0793	0.05757	0.07106	**0.01251**			0.0281	0.00028		0.00057		
λ_{11}									**0.03217**			
λ_{12}	0.00825				0.05672	0.0742	0.0632		**0.05285**			
λ_{13}								0.01748				0.00043
λ_{14}		0.01072	0.00491			0.0505					0.01504	
λ_{15}												
λ_{16}				**0.00648**	0.06162	0.00224				0.00779		0.03002
λ_{17}												
λ_{18}												
λ_{19}										0.00492		
λ_{20}			0.04684	**0.04161**		0.00249			**0.03813**		0.07388	0.01871
λ_{21}							0.07703	0.0569				
λ_{22}	0.01281				0.00472						0.0716	
λ_{23}		0.02557										
λ_{24}	0.19693	0.18061	0.16263	**0.17653**	0.16565	0.17721	0.11405	0.13916	**0.1512**	0.20131	0.07393	0.17667
ρ_7	0.00023	0.00814	0.03435	**0.01063**	0.00588	0.00111	0.01695	0.00933	**0.00657**	0.00328	0.00191	0.01326
ρ_8	0.99977	0.99186	0.96565	**0.98937**	0.99412	0.99889	0.98305	0.99067	**0.99343**	0.99672	0.99809	0.98674
Capacity	-11.65[dB]						-17.82[dB]					
$(E_b/N_0)^*$	-11.52[dB]						-17.67[dB]					

TABLE 2. Optimal degree distributions (λ^*, ρ^*) of rate-3/4 LDPC codes for multi-user massive MIMO system with MMSE-PIC for some candidate JDD strategies, where $(n_T \times n_R) = (4 \times 16)$ and (4×64) are considered, and $d_{v,\max} = 20$ is used.

$n_T \times n_R$	4×16						4×64					
$N_{det} : N_{dec}$	$1:1$	$1:2$	**$1:6$**	$1:8$	$1:14$	$3:1$	$1:1$	**$1:3$**	$1:5$	$1:6$	$1:8$	$3:1$
λ_2	0.23796	0.24379	**0.24071**	0.24009	0.24041	0.23996	0.2358	**0.23519**	0.23596	0.23564	0.23559	0.23559
λ_3	0.26839	0.20698	**0.2572**	0.26207	0.2628	0.26775	0.26229	**0.25645**	0.26081	0.26561	0.25497	0.2553
λ_4	0.00142	0.11727	**0.00887**	0.0007	0.01508	0.00101	0.00004	**0.01091**	0.00105	0.00113	0.00174	0.01819
λ_5												
λ_6	0.10691	0.0432	**0.1296**	0.1347	0.05537		0.13408	**0.14476**	0.10994	0.05117	0.1857	0.11328
λ_7						0.20585						
λ_8									0.27301	0.37086	0.07182	
λ_9	0.31241	0.07863	**0.19247**	0.27171	0.40998	0.1294	0.30972	**0.28479**				0.34803
λ_{10}		0.30339	**0.13207**								0.19867	
λ_{11}						0.14644	0.05281					
λ_{12}	0.04758			0.05631				**0.04427**	0.08256	0.04416		
λ_{13}								**0.01984**	0.03215		0.0511	0.01942
λ_{14}	0.02082	0.00523	**0.02772**	0.02741		0.00079	0.00173			0.00116		
λ_{15}					0.00042							0.00315
λ_{16}	0.00223			0.00582				**0.00191**	0.00254	0.02305	0.00007	
λ_{17}		0.0011			0.0074							
λ_{18}						0.00713	0.00285					0.00314
λ_{19}			**0.00083**		0.00153							
λ_{20}	0.00228	0.0004	**0.01054**	0.0012	0.00701	0.00168	0.00068	**0.00189**	0.00198	0.00721	0.00033	0.0039
ρ_{14}	0.00249	0.00315	**0.00076**	0.01741	0.01118	0.00126	0.0074	**0.00159**	0.01188	0.00065	0.00159	0.0007
ρ_{15}	0.99751	0.99685	**0.99924**	0.98259	0.98882	0.99874	0.9926	**0.99841**	0.98812	0.99935	0.99841	0.9993
Capacity	-10.05[dB]						-16.28[dB]					
$(E_b/N_0)^*$	-9.91[dB]						-16.20[dB]					

number of Gauss-Seidel iterations per each detection iteration is set as 1, i.e., $n_{GS} = 1$. Thus, we consider only $N_{det} : N_{dec}$ when designing a JDD strategy.

We solve the optimization problem (36) by using a differential evolution algorithm [50] with a concentrated check node degree distribution [30]. We find degree

TABLE 3. Optimal degree distributions (λ^*, ρ^*) of rate-1/2 LDPC codes for multi-user massive MIMO system with Approximate MMSE-PIC for some candidate JDD strategies, where ($n_T \times n_R$) = (4 × 16) and (4 × 64) are considered, and $d_{v,\max} = 24$ is used.

$n_T \times n_R$	4 × 16						4 × 64					
$N_{det} : N_{dec}$	1 : 1	1 : 5	1 : 6	**1 : 7**	2 : 1	3 : 1	1 : 1	1 : 2	**1 : 4**	1 : 5	1 : 9	2 : 1
λ_2	0.25359	0.25543	0.25411	**0.25467**	0.25241	0.25416	0.25099	0.24473	**0.24898**	0.2486	0.24943	0.24928
λ_3	0.20775	0.175	0.18783	**0.17446**	0.17891	0.17881	0.17322	0.2239	**0.19281**	0.19833	0.19066	0.19037
λ_4	0.01856	0.06313	0.00689	**0.04733**	0.05309	0.03494	0.06523	0.00418	**0.01216**	0.02683	0.03848	0.01098
λ_5	0.02006	0.05269	0.11751	**0.08943**	0.08281	0.10236	0.02964	0.00549	**0.1079**	0.05528	0.05301	0.11349
λ_6							0.13958					
λ_7	0.18863	0.1405	0.08966	**0.12339**	0.05964	0.12276		0.26161	**0.11416**	0.1332	0.1542	0.06345
λ_8	0.06181	0.02324	0.09741	**0.00232**	0.10474							0.12685
λ_9										0.10801		
λ_{10}	0.00504	0.03717		**0.05792**		0.04232	0.0901	0.04454	**0.09218**		0.1138	
λ_{11}												
λ_{12}	0.02651	0.01739	0.01175		0.03888					0.03416		
λ_{13}												
λ_{14}						0.03425	0.02484	0.00821	**0.03868**		0.005	0.00886
λ_{15}												
λ_{16}			0.00339				0.09011			0.00589		
λ_{17}											0.0084	
λ_{18}								0.02041	**0.03551**			
λ_{19}					0.02547	0.00139						0.11523
λ_{20}		0.0886		**0.08434**		0.09794		0.01207				0.02876
λ_{21}					0.07447							
λ_{22}	0.03646		0.01091	**0.1137**			0.05145		**0.0409**	0.04432	0.04059	
λ_{23}												
λ_{24}	0.18158	0.14683	0.22054	**0.05244**	0.12958	0.13107	0.08484	0.17485	**0.11672**	0.14538	0.14644	0.09272
ρ_7	0.02383	0.01839	0.0071	**0.00479**	0.01212	0.00734	0.02726	0.00281	**0.00098**	0.00056	0.00973	0.00652
ρ_8	0.97617	0.98161	0.9929	**0.99521**	0.98788	0.99266	0.97274	0.99719	**0.99902**	0.99944	0.99027	0.99348
Capacity	-11.65[dB]						-17.82[dB]					
$(E_b/N_0)^*$	-11.42[dB]						-17.62[dB]					

TABLE 4. Optimal degree distributions (λ^*, ρ^*) of rate-3/4 LDPC codes for multi-user massive MIMO system with Approximate MMSE-PIC for some candidate JDD strategies, where ($n_T \times n_R$) = (4 × 16) and (4 × 64) are considered, and $d_{v,\max} = 20$ is used.

$n_T \times n_R$	4 × 16						4 × 64					
$N_{det} : N_{dec}$	1 : 1	1 : 2	1 : 3	1 : 4	2 : 1	**3 : 6**	1 : 1	1 : 3	**1 : 6**	1 : 7	1 : 12	3 : 1
λ_2	0.24522	0.24514	0.24558	0.2459	0.24497	**0.24731**	0.23921	0.24038	**0.23777**	0.23791	0.23807	0.23871
λ_3	0.26348	0.26451	0.25699	0.25442	0.26445	**0.23088**	0.23485	0.20236	**0.25179**	0.25481	0.25401	0.24757
λ_4	0.01915	0.00022	0.01464	0.01778	0.00523	**0.06211**	0.03197	0.11157	**0.00138**	0.0011	0.00029	0.01322
λ_5												
λ_6		0.10245	0.10589	0.11457	0.0818	**0.09133**	0.19635	0.11871	**0.20924**	0.18377	0.20917	0.17118
λ_7												
λ_8	0.23568											
λ_9	0.09589	0.29807	0.21099	0.233	0.31213	**0.15247**	0.16044		**0.2097**	0.25867		0.26321
λ_{10}								0.28717			0.26491	
λ_{11}	0.09969		0.12738			**0.14755**		0.00243				
λ_{12}				0.10162	0.02242	**0.05226**	0.07776	0.03565			0.0211	0.02151
λ_{13}							0.05201					
λ_{14}		0.05314		0.00446	0.06272				**0.07378**	0.02827	0.0111	0.03296
λ_{15}	0.02906	0.02358							**0.01006**			
λ_{16}			0.02914	0.00482	0.00611				**0.00242**			
λ_{17}	0.01026	0.00619								0.02587		0.00057
λ_{18}			0.00681								0.00047	
λ_{19}						**0.00619**	0.0019	0.00055		0.00522		
λ_{20}	0.00157	0.00672	0.00258	0.02342	0.00017	**0.0099**	0.00551	0.00119	**0.00387**	0.00439	0.00088	0.01108
ρ_{14}	0.00252	0.00296	0.00789	0.03513	0.00172	**0.00357**	0.00017	0.00078	**0.02203**	0.00382	0.00118	0.01637
ρ_{15}	0.99748	0.99704	0.99211	0.96487	0.99828	**0.99643**	0.99983	0.99922	**0.97797**	0.99618	0.99882	0.98363
Capacity	-10.05[dB]						-16.28[dB]					
$(E_b/N_0)^*$	-9.88[dB]						-16.19[dB]					

distributions ($\boldsymbol{\lambda}^*$, $\boldsymbol{\rho}^*$) achieving the threshold $(E_b/N_0)^*$ with different JDD strategies for each channel scenario and code rate under consideration. Then, we determine the overall optimal degree distribution ($\boldsymbol{\lambda}^\dagger$, $\boldsymbol{\rho}^\dagger$) among candidate ($\boldsymbol{\lambda}^*$, $\boldsymbol{\rho}^*$) resulting in the fastest JDD convergence.

TABLE 5. Optimal degree distributions (λ^*, ρ^*) of rate-1/2 LDPC codes for multi-user massive MIMO system with Gauss-Seidel-aided MMSE-PIC for some candidate JDD strategies, where ($n_T \times n_R$) = (4 × 16) and (4 × 64) are considered, and $d_{v,\max} = 24$ is used.

$n_T \times n_R$	4 × 16						4 × 64					
$N_{det} : N_{dec}$	1 : 1	1 : 2	1 : 4	1 : 6	**1 : 7**	1 : 12	1 : 1	1 : 3	1 : 7	**1 : 9**	2 : 1	4 : 1
λ_2	0.24632	0.24929	0.24715	0.24518	**0.24594**	0.24627	0.24383	0.24558	0.24194	**0.24509**	0.24124	0.24433
λ_3	0.19762	0.15482	0.18818	0.19943	**0.20293**	0.17363	0.20529	0.20122	0.20942	**0.2075**	0.19651	0.19778
λ_4	0.01925	0.1064	0.0083	0.01828	**0.02317**	0.02279	0.01847	0.03901	0.00761	**0.01165**	0.05668	0.00788
λ_5	0.08651	0.0629	0.11501	0.09192	**0.05239**	0.16262	0.05863	0.01827	0.07841	**0.06336**	0.03768	0.10838
λ_6						0.03567						0.05009
λ_7	0.09467	0.02131	0.18465	0.06863	**0.17189**		0.1733	0.20231	0.14834	**0.12294**	0.11107	
λ_8	0.08039	0.16219		0.13517	**0.06677**	0.06117	0.03733		0.06663	**0.11499**	0.11832	0.13838
λ_9												
λ_{10}	0.04971					0.06847		0.07613				
λ_{11}												
λ_{12}												
λ_{13}							0.08522	0.00001	0.05633	**0.0044**		
λ_{14}	0.04989	0.01294	0.01947		**0.00748**			0.0467				0.01281
λ_{15}			0.00374	0.03971					0.00573	**0.05571**		
λ_{16}		0.04443										0.0957
λ_{17}				0.06256					0.00786		0.05717	
λ_{18}			0.08192			0.07925					0.03913	
λ_{19}					**0.08958**	0.01796						
λ_{20}	0.01416	0.10011		0.0032	**0.07013**							
λ_{21}												
λ_{22}			0.12485				0.09686			**0.06551**		0.04066
λ_{23}							0.0184	0.05808			0.13241	
λ_{24}	0.16147	0.08561	0.02673	0.1359	**0.06971**	0.13217	0.06269	0.11268	0.17773	**0.10885**	0.00977	0.10398
ρ_7	0.00409	0.02258	0.00987	0.01091	**0.02826**	0.00596	0.01235	0.00198	0.00897	**0.01483**	0.00295	0.00599
ρ_8	0.99591	0.97742	0.99013	0.98909	**0.97174**	0.99404	0.98765	0.99802	0.99103	**0.98517**	0.99705	0.99401
Capacity	-11.65[dB]						-17.82[dB]					
$(E_b/N_0)^*$	-11.61[dB]						-17.70[dB]					

TABLE 6. Optimal degree distributions (λ^*, ρ^*) of rate-3/4 LDPC codes for multi-user massive MIMO system with Gauss-Seidel-aided MMSE-PIC for some candidate JDD strategies, where ($n_T \times n_R$) = (4 × 16) and (4 × 64) are considered, and $d_{v,\max} = 20$ is used.

$n_T \times n_R$	4 × 16						4 × 64					
$N_{det} : N_{dec}$	1 : 1	1 : 2	1 : 3	1 : 4	**1 : 13**	2 : 1	1 : 1	1 : 2	1 : 5	**1 : 8**	1 : 10	2 : 4
λ_2	0.23538	0.23394	0.23637	0.23561	**0.23558**	0.23386	0.23315	0.23364	0.23258	**0.23191**	0.23299	0.23479
λ_3	0.23995	0.26139	0.22892	0.23911	**0.21445**	0.26473	0.25321	0.26005	0.25743	**0.26513**	0.26694	0.21789
λ_4	0.04828	0.00924	0.00984	0.01463	**0.07925**	0.00334	0.01856	0.00269	0.00088	**0.0039**	0.00124	0.10649
λ_5												
λ_6	0.13467	0.12719	0.32683	0.25618	**0.18661**	0.12309	0.13171	0.15048	0.2103	**0.12547**	0.06083	
λ_7												
λ_8												0.2774
λ_9	0.27416	0.35602		0.06622		0.36953	0.34144	0.31194		**0.35823**	0.37444	0.08627
λ_{10}					**0.18238**				0.2902			
λ_{11}	0.05466			0.16307	**0.07965**							
λ_{12}			0.08027			0.0007						
λ_{13}			0.10326		**0.01267**			0.03988	0.00246			0.07232
λ_{14}			0.00094				0.00649		0.00396	**0.00389**	0.05533	
λ_{15}		0.00034			**0.00602**	0.0013						0.00352
λ_{16}	0.00227	0.00512								**0.00704**	0.00079	
λ_{17}		0.00622	0.00886									
λ_{18}	0.0007			0.00648		0.00092	0.01172	0.00007		**0.00326**	0.0018	0.00102
λ_{19}				0.009			0.00306	0.00041	0.00066			
λ_{20}	0.00992	0.00053	0.0047	0.00969	**0.00339**	0.00253	0.00066	0.00086	0.00153	**0.00118**	0.00562	0.00029
ρ_{14}	0.04615	0.00131	0.00316	0.00814	**0.0008**	0.00255	0.00101	0.00132	0.00814	**0.00204**	0.00665	0.00394
ρ_{15}	0.95385	0.99869	0.99684	0.99186	**0.9992**	0.99745	0.99899	0.99868	0.99186	**0.99796**	0.99335	0.99606
Capacity	-10.05[dB]						-16.28[dB]					
$(E_b/N_0)^*$	-10.02[dB]						-16.17[dB]					

In Table 1 - Table 6, we list degree distributions ($\boldsymbol{\lambda}^*$, $\boldsymbol{\rho}^*$) of LDPC codes for multi-user massive MIMO systems achieving the threshold by some candidate JDD strategies for each channel scenario, code rate and detection algorithm under consideration. By a practical reason, λ_{d_v} and ρ_{d_c} having negligible values are enforced to be null. In each table,

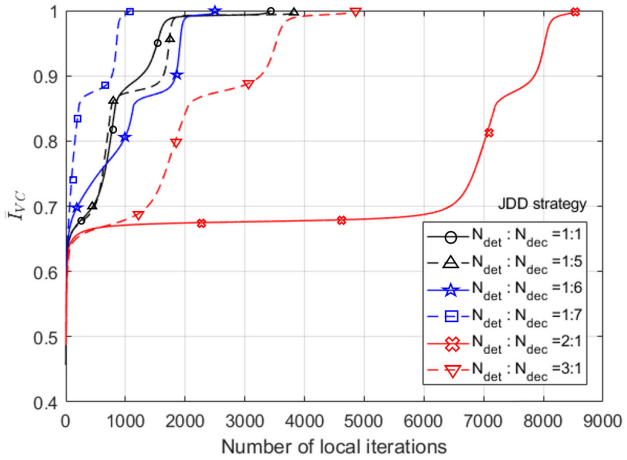

FIGURE 7. Evolution of $\bar{I}_{VC}$ with respect to the number of local iterations for some JDD strategies with Approximate MMSE-PIC detection, where $R = 1/2$, $n_T = 4$, $n_R = 16$.

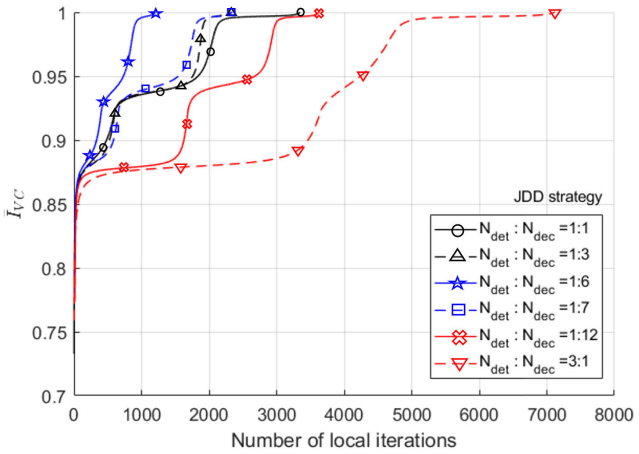

FIGURE 8. Evolution of $\bar{I}_{VC}$ with respect to the number of local iterations for some JDD strategies with Approximate MMSE-PIC detection, where $R = 3/4$, $n_T = 4$, $n_R = 64$.

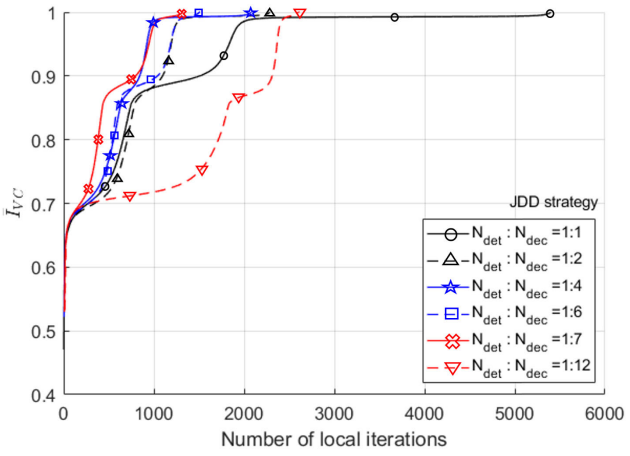

FIGURE 9. Evolution of $\bar{I}_{VC}$ with respect to the number of local iterations for some JDD strategies with Gauss-Seidel-aided MMSE-PIC detection, where $R = 1/2$, $n_T = 4$, $n_R = 16$.

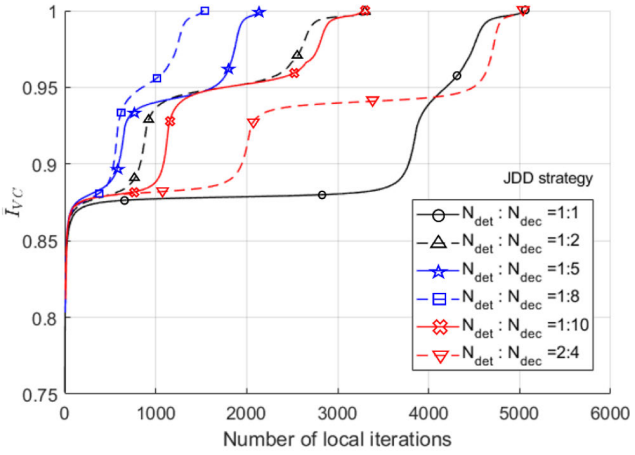

FIGURE 10. Evolution of $\bar{I}_{VC}$ with respect to the number of local iterations for some JDD strategies with Gauss-Seidel-aided MMSE-PIC detection, where $R = 3/4$, $n_T = 4$, $n_R = 64$.

we also list the channel capacity and the threshold obtained by EXIT analysis. It is observed that for a given channel scenario, the threshold is obtained identically irrespective of the JDD strategy. This implies that equivalent error correcting capabilities are attained by different JDD strategies if an infinite number of iterations are allowed, although distinct JDD strategies result in different convergence speeds as will be shown below.

In Fig. 5 - Fig. 10, we plot evolutions of $\bar{I}_{VC}$ with respect to the number of local iterations obtained at the threshold E_b/N_0 by some candidate JDD strategies for given channel scenario, code rate and detection algorithm. Evolution curves are obtained by EXIT analysis for multi-user massive MIMO system using LDPC codes whose degree distributions are listed in Table 1 - Table 6. A faster evolution of $\bar{I}_{VC}$ toward 1 indicates a faster convergence of JDD algorithm. Taking 3-D EXIT chart obtained at just above the threshold E_b/N_0 into consideration, it is obvious that the JDD trajectory penetrates a tunnel formed between two EXIT surfaces by a high number of small strides of zig-zag movements. This may explain the reason why $\bar{I}_{VC}$ converges to 1 after a high number of local iterations at the threshold E_b/N_0 as shown in Fig. 5 - Fig. 10. We plot in Fig. 11 evolutions of $\bar{I}_{VC}$ obtained at some different values of E_b/N_0 for the same scenario as in Fig. 7. It is observed from Fig. 7 and Fig. 11 that at higher E_b/N_0, $\bar{I}_{VC}$ converges to 1 with a lower number of local iterations. This implies that a tunnel formed between two EXIT surfaces is wide open so that the JDD trajectory penetrates the tunnel and reaches the convergent point with a small number of zig-zag movements. Distinct JDD strategies sequentially result in different degree distributions, different shapes of EXIT surfaces, different shapes of tunnel and different JDD trajectories, and consequently different JDD convergence speeds.

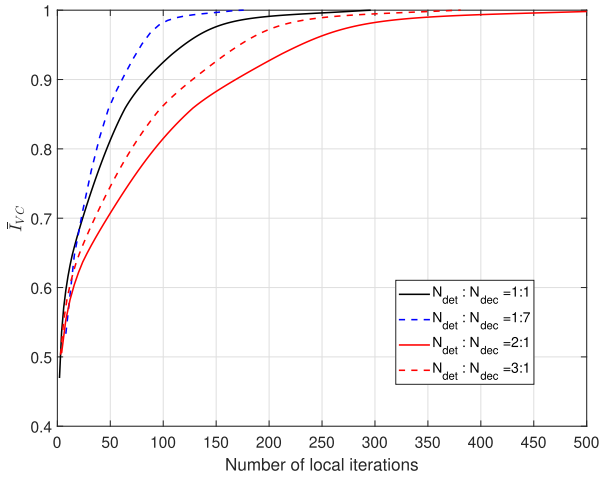

(a) $E_b/N_0 = -11.2$dB

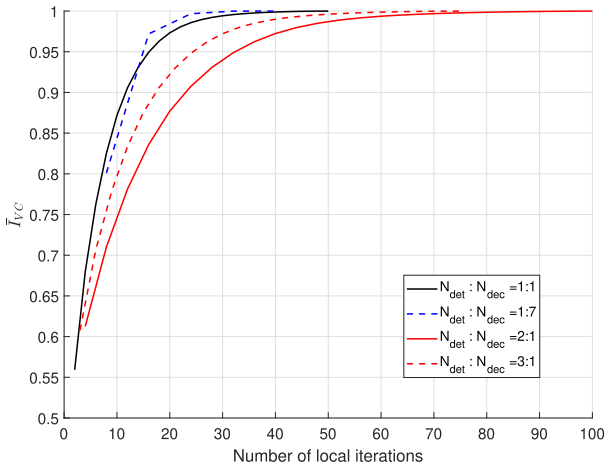

(b) $E_b/N_0 = -9.7$dB

FIGURE 11. Evolution of $\bar{I}_{VC}$ with respect to the number of local iterations obtained for various values of E_b/N_0 with Approximate MMSE-PIC detection, where $R = 1/2$, $n_T = 4$, $n_R = 16$.

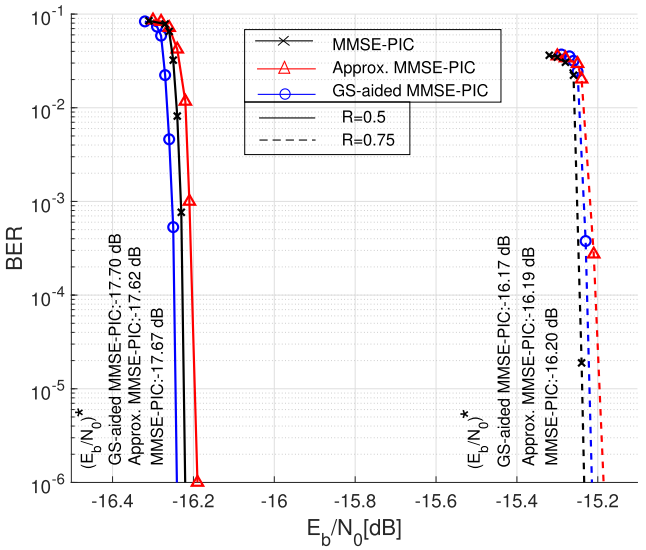

FIGURE 12. BER of LDPC coded multi-user massive MIMO system with $N = 64000$, $n_T = 4$ and $n_R = 64$, where the number of local iterations is high enough to result in the convergence of JDD.

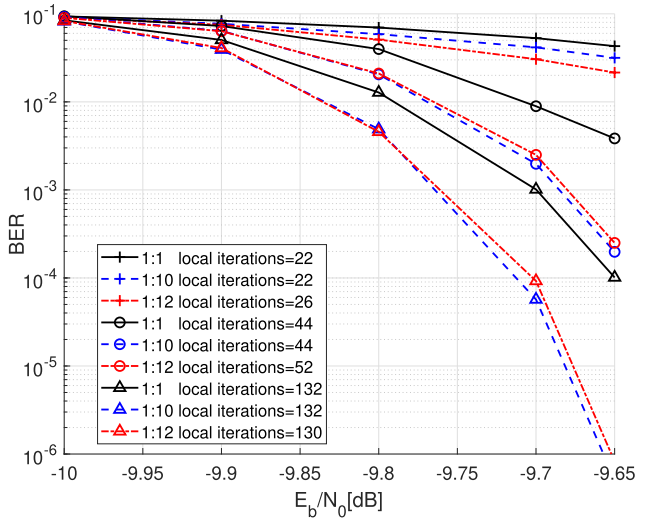

FIGURE 13. BER of rate-1/2 LDPC coded multi-user massive MIMO system using MMSE-PIC detection with $N = 2304$ over 4×16 channel obtained by different JDD strategies and different numbers of local iterations.

In each of Table 1 - Table 6, we mark the optimal JDD strategy and values of overall optimal degree distributions $(\boldsymbol{\lambda}^\dagger, \boldsymbol{\rho}^\dagger)$ by boldface fonts. It is observed that the optimal JDD strategy differs from $N_{det} : N_{dec} = 1 : 1$ which has been widely used in conventional schemes. The optimal JDD strategy varies depending on the channel scenario, code rate and detection algorithm. It is obvious that the proposed analysis tool enables us to choose the optimal JDD strategy very easily and efficiently depending on the environment encountered by the system. Some of previous works adopt non-conventional JDD strategies [18], [19], [20], but the choice of JDD strategy is not environment-dependent and the rationale of the choice for JDD strategy is not clearly presented. In this aspect, we claim that the proposed EXIT analysis tool is very useful and practical in the multi-user massive-MIMO communication system.

We construct parity-check matrices of LDPC codes of specific blocklengths N by applying PEG algorithm [49] to realize target degree distributions $(\boldsymbol{\lambda}^*, \boldsymbol{\rho}^*)$. Then, we perform BER simulations for coded multi-user massive MIMO system with various JDD strategies for each code rate, channel scenario and detection algorithm. In Fig. 12, we plot the BER of coded multi-user massive MIMO system using various MMSE-PIC detection algorithms in JDD process, where accordingly optimal JDD strategies and optimally designed LDPC codes with sufficiently long blocklength, i.e., $N = 64000$, are employed. It is observed that the order of threshold values for various schemes predicted by EXIT analysis matches well the order of BER performances obtained by simulations, although threshold value itself is a little bit distant from the simulated result. This verifies the practical effectiveness of the proposed EXIT analysis in designing the coded multi-user massive MIMO systems.

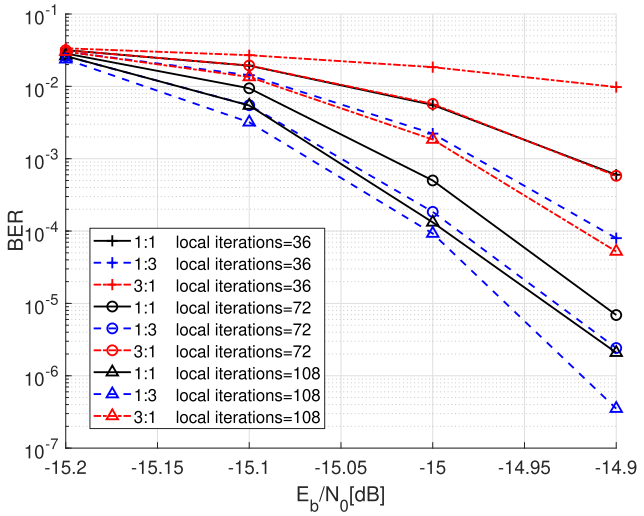

FIGURE 14. BER of rate-3/4 LDPC coded multi-user massive MIMO system using MMSE-PIC detection with $N = 4096$ over 4×64 channel obtained by different JDD strategies and different numbers of local iterations.

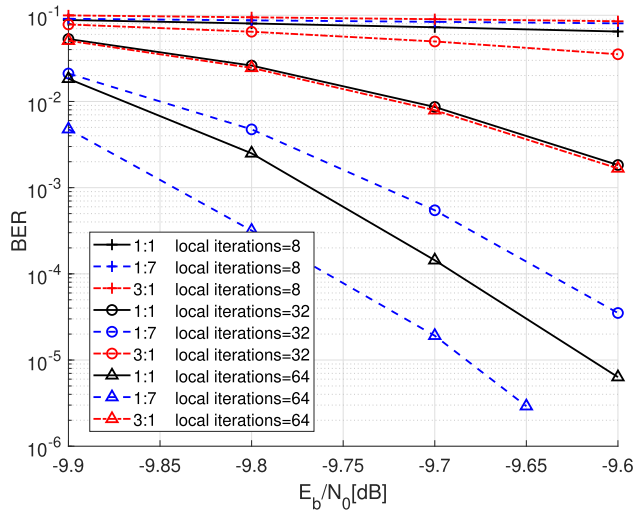

FIGURE 15. BER of rate-1/2 LDPC coded multi-user massive MIMO system using Approximate MMSE-PIC detection with $N = 2304$ over 4×16 channel obtained by different JDD strategies and different numbers of local iterations.

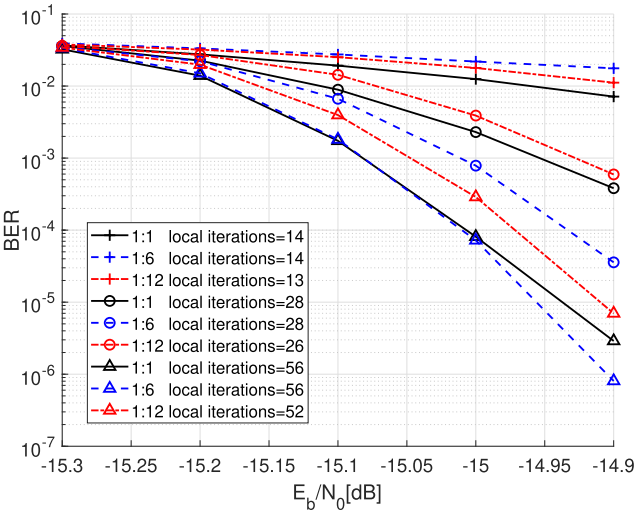

FIGURE 16. BER of rate-3/4 LDPC coded multi-user massive MIMO system using Approximate MMSE-PIC detection with $N = 4096$ over 4×64 channel obtained by different JDD strategies and different numbers of local iterations.

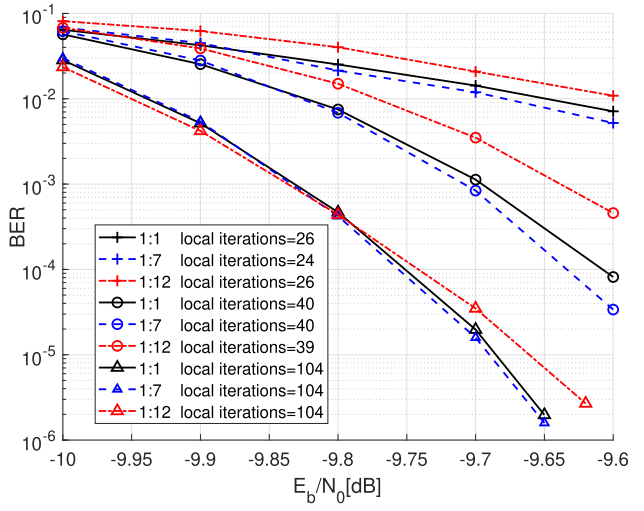

FIGURE 17. BER of rate-1/2 LDPC coded multi-user massive MIMO system using Gauss-Seidel-aided MMSE-PIC detection with $N = 2304$ over 4×16 channel obtained by different JDD strategies and different numbers of local iterations.

In Fig. 13 - Fig. 18, we plot BER performances of LDPC coded multi-user massive MIMO system with short to medium blocklength, whose LDPC codes are constructed by degree distributions $(\boldsymbol{\lambda}^*, \boldsymbol{\rho}^*)$ listed in Table 1 - Table 6 with the PEG algorithm. In each figure, we plot BER performances obtained by three candidate JDD strategies chosen from each corresponding table. Note that JDD candidates used in Fig. 13 are chosen from Table 1 and the corresponding convergence behaviors of $\bar{I}_{VC}$ are presented in Fig. 5. In this manner, each of the following triplets are associated with one another: (Fig. 6, Fig. 14, Table 2), (Fig.7, Fig. 15, Table 3), (Fig. 8, Fig. 16, Table 4), (Fig. 9, Fig. 17, Table 5), and (Fig. 10, Fig. 18, Table 6). In each of Fig. 13 - Fig. 18, we compare BERs of distinct JDD strategies obtained by the same or similar numbers of local iterations. For this purpose, we choose common multiples of $N_{det} + N_{dec}$ of JDD strategies under comparison as local iteration numbers at which BERs are read and compared. In case that a common multiple is not found, multiples of $N_{det} + N_{dec}$ having similar values are chosen as local iteration numbers to be tested. We pick up three groups of local iteration numbers, each of which corresponds to a beginning stage, a middle stage and a converging stage, respectively, of the BER evolution. Then, we plot BERs obtained at three different groups of local iteration numbers as in Fig. 13 - Fig. 18. By investigating these figures, we can compare the convergence speeds of JDD algorithm obtained by distinct JDD strategies. It is clear that the convergence speed of JDD can be predicted well by using

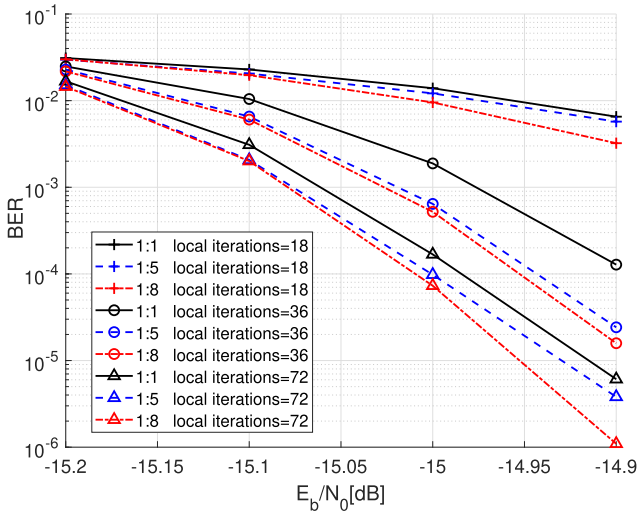

FIGURE 18. BER of rate-3/4 LDPC coded multi-user massive MIMO system using Gauss-Seidel-aided MMSE-PIC detection with $N = 4096$ over 4×64 channel obtained by different JDD strategies and different numbers of local iterations.

the evolution of $\bar{I}_{VC}$ based on the proposed EXIT analysis. For example, in Fig. 15, BER curves drawn with dashed lines corresponding to the JDD strategy of 1:7 improves the most rapidly among three JDD strategies under comparison, which is consistent with the prediction made from Fig. 7. It is also clear that using the optimal JDD strategy and overall optimal degree distribution $(\boldsymbol{\lambda}^{\dagger}, \boldsymbol{\rho}^{\dagger})$ results in the lowest BER for a given number of local iterations, or equivalently, the fastest convergence of JDD for each channel scenario, code rate and detection algorithm. We may also compare convergence speeds of JDD strategies by using BER evolution curves obtained with respect to the number of local iterations as depicted in Fig. 19 and Fig. 20. These two figures are obtained by tracing BERs given in Fig. 15 and Fig. 18, respectively, with respect to the local iteration number at particular values of E_b/N_0. Note that different BER evolution curves are obtained at different E_b/N_0 as shown in Fig. 19. In order to compare convergence speeds of JDD strategies over a wide range of E_b/N_0, BER evolution curves at many different values of E_b/N_0 need to be obtained, which is not efficient. Thus, alternatively, we plot BER curves as in Fig. 13 - Fig. 18 to compare convergence speeds of JDD strategies over all E_b/N_0.

We compare performances of LDPC coded multi-user massive MIMO systems obtained by using different detection algorithms in JDD, i.e., MMSE-PIC, Approximate MMSE-PIC and Gauss-Seidel-aided MMSE-PIC, where optimal JDD strategies found for each case are used. By revisiting Fig. 12, we find that three detection algorithms result in similar values of threshold and similar BER performances with sufficiently long blocklength. However, these detection schemes show distinct convergence speeds. It is predicted from Fig. 21 that the use of Approximate MMSE-PIC results in the fastest JDD convergence while we obtain the slowest convergence

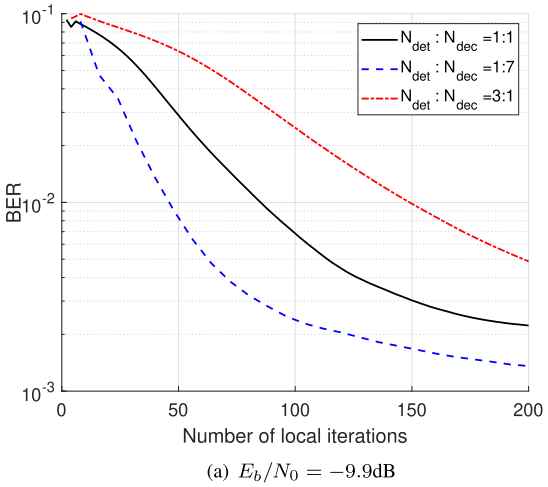

(a) $E_b/N_0 = -9.9$dB

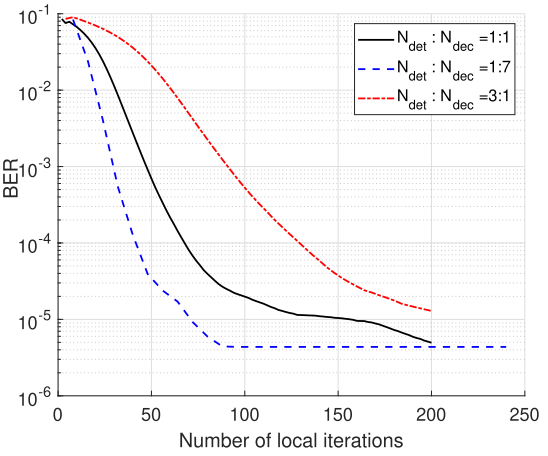

(b) $E_b/N_0 = -9.7$dB

FIGURE 19. BER of rate-1/2 LDPC coded multi-user massive MIMO system with $N = 2304$ over 4×16 channel obtained by using Approximate MMSE-PIC detection at particular E_b/N_0.

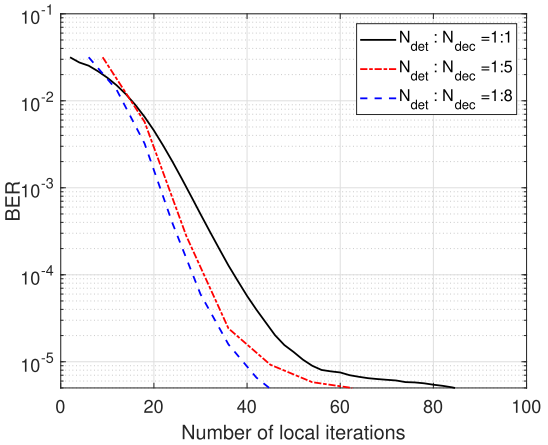

FIGURE 20. BER of rate-3/4 LDPC coded multi-user massive MIMO system with $N = 4096$ over 4×64 channel obtained by using Gauss-Seidel-aided MMSE-PIC detection at $E_b/N_0 = -14.9$dB.

behavior by using MMSE-PIC detection. This prediction is confirmed by simulations as shown in Fig. 22. Note that BER performances presented in Fig. 22 are obtained

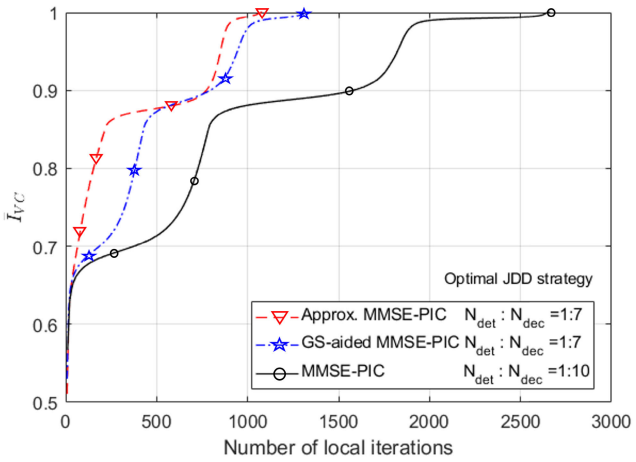

FIGURE 21. Evolution of $\bar{I}_{VC}$ with respect to the number of local iterations with MMSE-PIC, Approximate MMSE-PIC and Gauss-Seidel-aided MMSE-PIC detection algorithms, where $R = 1/2$, $n_T = 4$, $n_R = 16$.

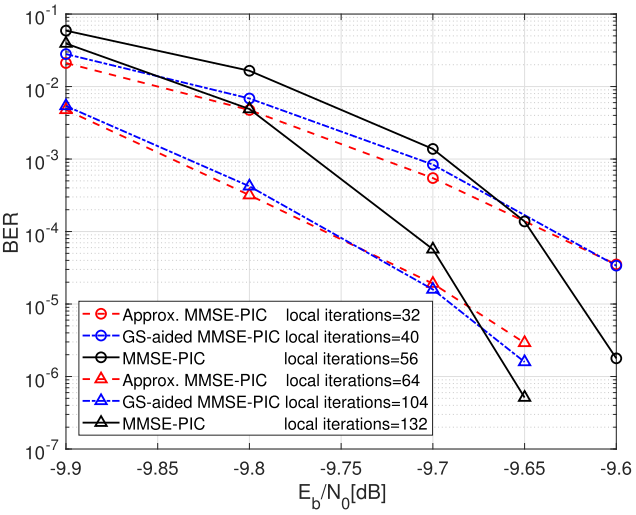

FIGURE 22. BER of rate-1/2 LDPC coded multi-user massive MIMO system with $N = 2304$ over 4×16 channel obtained by using MMSE-PIC, Approximate MMSE-PIC and Gauss-Seidel-aided MMSE-PIC detection algorithms.

with short blocklength, where MMSE-PIC outperforms other detection algorithms at high E_b/N_0 and BER curves experience a cross-over in the intermediate E_b/N_0 region. We can state that a reasonably good BER performance is obtained by using Approximate MMSE-PIC or Gauss-Seidel-aided MMSE-PIC detection algorithms with a lower number of iterations and consequently with higher throughputs. It follows that in the communication environment with higher target throughput, Approximate MMSE-PIC can be a good choice for the detection algorithm in the JDD process of LDPC coded multi-user massive-MIMO system.

VII. CONCLUSION

In this paper, we proposed an efficient analysis tool for investigating the JDD behavior of LDPC coded multi-user massive MIMO system employing MMSE-PIC detection and its variations as a low-complexity linear detection algorithm. For this purpose, we provided a factor graph representation of LDPC coded multi-user massive MIMO system and formulated message updating processes in the iterative JDD process. Then, we defined an EXIT characteristics of component units in the overall system and analyzed the behavior of JDD process in terms of EXIT mechanism. Then, we designed jointly LDPC codes and the JDD strategy in order to achieve a lower BER and a faster convergence speed of JDD process. It was verified that the proposed analysis tool can predict the error correcting capability and the JDD convergence behavior quite well and thus the proposed tool is useful for designing LDPC coded multi-user massive MIMO system. It was also confirmed that the system designed optimally by the proposed analysis tool achieves a lower BER with a faster convergence speed.

REFERENCES

[1] E. Telatar, "Capacity of multi-antenna Gaussian channels," *Eur. Trans. Telecommun.*, vol. 10, no. 6, pp. 585–595, Feb. 1999.
[2] J. Mietzner, R. Schober, L. Lampe, W. H. Gerstacker, and P. A. Hoeher, "Multiple-antenna techniques for wireless communications—A comprehensive literature survey," *IEEE Commun. Surveys Tuts.*, vol. 11, no. 2, pp. 87–105, 2nd Quart., 2009.
[3] F. Rusek, D. Persson, B. K. Lau, E. G. Larsson, T. L. Marzetta, O. Edfors, and F. Tufvesson, "Scaling up MIMO: Opportunities and challenges with very large arrays," *IEEE Signal Process. Mag.*, vol. 30, no. 1, pp. 40–60, Jan. 2013.
[4] E. G. Larsson, O. Edfors, F. Tufvesson, and T. L. Marzetta, "Massive MIMO for next generation wireless systems," *IEEE Commun. Mag.*, vol. 52, no. 2, pp. 186–195, Feb. 2014.
[5] X. Ge, S. Tu, G. Mao, C.-X. Wang, and T. Han, "5G ultra-dense cellular networks," *IEEE Wireless Commun.*, vol. 23, no. 1, pp. 72–79, Feb. 2016.
[6] W. H. Chin, Z. Fan, and R. Haines, "Emerging technologies and research challenges for 5G wireless networks," *IEEE Wireless Commun.*, vol. 21, no. 2, pp. 106–112, Apr. 2014.
[7] E. G. Larsson, "Massive MIMO for 5G: Overview and the road ahead," in *Proc. 51st Annu. Conf. Inf. Sci. Syst. (CISS)*, Baltimore, MD, USA, Mar. 2017, p. 1.
[8] J. Zuo, J. Zhang, C. Yuen, W. Jiang, and W. Luo, "Multicell multiuser massive MIMO transmission with downlink training and pilot contamination precoding," *IEEE Trans. Veh. Technol.*, vol. 65, no. 8, pp. 6301–6314, Aug. 2016.
[9] X. Ge, R. Zi, H. Wang, J. Zhang, and M. Jo, "Multi-user massive MIMO communication systems based on irregular antenna arrays," *IEEE Trans. Wireless Commun.*, vol. 15, no. 8, pp. 5287–5301, Aug. 2016.
[10] S. Yoon and C.-B. Chae, "Low-complexity MIMO detection based on belief propagation over pairwise graphs," *IEEE Trans. Veh. Technol.*, vol. 63, no. 5, pp. 2363–2377, Jun. 2014.
[11] P. Som, T. Datta, N. Srinidhi, A. Chockalingam, and B. S. Rajan, "Low-complexity detection in large-dimension MIMO-ISI channels using graphical models," *IEEE J. Sel. Topics Signal Process.*, vol. 5, no. 8, pp. 1497–1511, Dec. 2011.
[12] H. Q. Ngo, M. Matthaiou, T. Q. Duong, and E. G. Larsson, "Uplink performance analysis of multicell MU-SIMO systems with ZF receivers," *IEEE Trans. Veh. Technol.*, vol. 62, no. 9, pp. 4471–4483, Nov. 2013.
[13] M. Matthaiou, C. Zhong, M. R. McKay, and T. Ratnarajah, "Sum rate analysis of ZF receivers in distributed MIMO systems," *IEEE J. Sel. Areas Commun.*, vol. 31, no. 2, pp. 180–191, Feb. 2013.
[14] Y.-C. Liang, G. Pan, and Z. D. Bai, "Asymptotic performance of MMSE receivers for large systems using random matrix theory," *IEEE Trans. Inf. Theory*, vol. 53, no. 11, pp. 4173–4190, Nov. 2007.
[15] X. Gao, L. Dai, C. Yuen, and Y. Zhang, "Low-complexity MMSE signal detection based on Richardson method for large-scale MIMO systems," in *Proc. IEEE 80th Veh. Technol. Conf. (VTC-Fall)*, Vancouver, BC, Canada, Sep. 2014, pp. 1–5.
[16] I. A. Khoso, X. Dai, M. N. Irshad, A. Khan, and X. Wang, "A low complexity data detection algorithm for massive MIMO systems," *IEEE Access*, vol. 7, pp. 39341–39351, 2019.

[17] L. Fang, L. Xu, and D. Huang, "Low complexity iterative MMSE-PIC detection for medium-size massive MIMO, *IEEE Wireless Commun. Lett.*, vol. 5, no. 1, pp. 108–111, Feb. 2016.
[18] W.-C. Sun, W.-H. Wu, C.-H. Yang, and Y.-L. Ueng, "An iterative detection and decoding receiver for LDPC-coded MIMO systems," *IEEE Trans. Circuits Syst. I, Reg. Papers*, vol. 62, no. 10, pp. 2512–2522, Oct. 2015.
[19] W.-C. Sun, Y.-C. Su, Y.-L. Ueng, and C.-H. Yang, "An LDPC-coded SCMA receiver with multi-user iterative detection and decoding," *IEEE Trans. Circuits Syst. I, Reg. Papers*, vol. 66, no. 9, pp. 3571–3584, Sep. 2019.
[20] M. Zhang and S. Kim, "Evaluation of MMSE-based iterative soft detection schemes for coded massive MIMO system," *IEEE Access*, vol. 7, pp. 10166–10175, 2019.
[21] B. Cheng, Y. Shen, H. Wang, Z. Zhang, X. You, and C. Zhang, "Efficient MMSE-PIC detection for polar-coded system using tree-structured gray codes," *IEEE Wireless Commun. Lett.*, vol. 11, no. 7, pp. 1310–1314, Jul. 2022.
[22] C. Tang, C. Liu, L. Yuan, and Z. Xing, "High precision low complexity matrix inversion based on Newton iteration for data detection in the massive MIMO," *IEEE Commun. Lett.*, vol. 20, no. 3, pp. 490–493, Mar. 2016.
[23] L. Dai, X. Gao, X. Su, S. Han, I. Chih-Lin, and Z. Wang, "Low-complexity soft-output signal detection based on Gauss–Seidel method for uplink multiuser large-scale MIMO systems," *IEEE Trans. Veh. Technol.*, vol. 64, no. 10, pp. 4839–4845, Oct. 2015.
[24] R. G. Gallager, *Low-Density Parity-Check Codes*. Cambridge, MA, USA: MIT Press, 1963.
[25] T. J. Richardson and R. L. Urbanke, "The capacity of low-density parity-check codes under message-passing decoding," *IEEE Trans. Inf. Theory*, vol. 47, no. 2, pp. 599–618, Feb. 2001.
[26] T. J. Richardson, M. A. Shokrollahi, and R. L. Urbanke, "Design of capacity-approaching irregular low-density parity-check codes," *IEEE Trans. Inf. Theory*, vol. 47, no. 2, pp. 619–637, Feb. 2001.
[27] *IEEE Standard for Local and Metropolitan Area Networks, Part 16: Air Interface for Broadband Wireless Access Systems*, Standard 802.16TM-2009, May 2009.
[28] *Digital Video Broadcasting (DVB); Second Generation Framing Structure, Channel Coding and Modulation Systems for Broadcasting, Interactive Services, News Gathering and Other Broadband Satellite Applications (DVB-S2)*, Standard ETSI Standard EN 302 307, European Telecommunications Standards Institute, Valbonne, France, 2005.
[29] *IEEE P802.3ca 50G-EPON Task Force*. Accessed: Jul. 2020. [Online]. Available: http://www.ieee802.org/3/ca/
[30] S.-Y. Chung, T. J. Richardson, and R. L. Urbanke, "Analysis of sum-product decoding of low-density parity-check codes using a Gaussian approximation," *IEEE Trans. Inf. Theory*, vol. 47, no. 2, pp. 657–670, Feb. 2001.
[31] S. ten Brink, "Convergence behavior of iteratively decoded parallel concatenated codes," *IEEE Trans. Commun.*, vol. 49, no. 10, pp. 1727–1737, Oct. 2001.
[32] S. ten Brink, G. Kramer, and A. Ashikhmin, "Design of low-density parity-check codes for modulation and detection," *IEEE Trans. Commun.*, vol. 52, no. 4, pp. 670–678, Apr. 2004.
[33] A. G. D. Uchoa, C. T. Healy, and R. C. de Lamare, "Iterative detection and decoding algorithms for MIMO systems in block-fading channels using LDPC codes," *IEEE Trans. Veh. Technol.*, vol. 65, no. 4, pp. 2735–2741, Apr. 2016.
[34] B. Lu, G. Yue, and X. Wang, "Performance analysis and design optimization of LDPC-coded MIMO OFDM systems," *IEEE Trans. Signal Process.*, vol. 52, no. 2, pp. 348–361, Feb. 2004.
[35] J. Zheng and B. D. Rao, "LDPC-coded MIMO systems with unknown block fading channels: Soft MIMO detector design, channel estimation, and code optimization," *IEEE Trans. Signal Process.*, vol. 54, no. 4, pp. 1504–1518, Apr. 2006.
[36] I. Hwang, H. Park, and J. Lee, "LDPC coded massive MIMO systems," *Entropy*, vol. 21, no. 3, p. 231, Feb. 2019.
[37] H. J. Park and J. W. Lee, "LDPC coded multi-user massive MIMO systems with low-complexity detection," *IEEE Access*, vol. 10, pp. 25296–25308, 2022.
[38] Y. Chi, L. Liu, G. Song, Y. Li, Y. L. Guan, and C. Yuen, "Constrained capacity optimal generalized multi-user MIMO: A theoretical and practical framework," *IEEE Trans. Commun.*, vol. 70, no. 12, pp. 8086–8104, Dec. 2022.
[39] Q. Liu, Z. Feng, J. Xu, Z. Zhang, W. Liu, and H. Ding, "Optimization of non-binary LDPC coded massive MIMO systems with partial mapping and REP detection," *IEEE Access*, vol. 10, pp. 17933–17945, 2022.
[40] T. V. Nguyen, "Optimized uniform scalar quantizers of ternary ADCs for large-scale MIMO communications," *IEEE Access*, vol. 9, pp. 94756–94768, 2021.
[41] D. Verenzuela, E. Björnson, X. Wang, M. Arnold, and S. ten Brink, "Massive-MIMO iterative channel estimation and decoding (MICED) in the uplink," *IEEE Trans. Commun.*, vol. 68, no. 2, pp. 854–870, Feb. 2020.
[42] T. V. Nguyen, H. D. Vu, D. N. Nguyen, and H. T. Nguyen, "Performance analysis of protograph LDPC codes over large-scale MIMO channels with low-resolution ADCs," *IEEE Access*, vol. 7, pp. 145145–145160, 2019.
[43] H. D. Vu, T. V. Nguyen, D. N. Nguyen, and H. T. Nguyen, "On design of protograph LDPC codes for large-scale MIMO systems," *IEEE Access*, vol. 8, pp. 46017–46029, 2020.
[44] H. N. Dang, H. T. Nguyen, and T. V. Nguyen, "Joint detection and decoding of mixed-ADC large-scale MIMO communication systems with protograph LDPC codes," *IEEE Access*, vol. 9, pp. 101013–101029, 2021.
[45] P. Suthisopapan, K. Kasai, A. Meesomboon, and V. Imtawil, "Achieving near capacity of non-binary LDPC coded large MIMO systems with a novel ultra low-complexity soft-output detector," *IEEE Trans. Wireless Commun.*, vol. 12, no. 10, pp. 5185–5199, Oct. 2013.
[46] T. L. Narasimhan and A. Chockalingam, "EXIT chart based design of irregular LDPC codes for large-MIMO systems," *IEEE Commun. Lett.*, vol. 17, no. 1, pp. 115–118, Jan. 2013.
[47] T. L. Narasimhan and A. Chockalingam, "Detection and decoding in large-scale MIMO systems: A non-binary belief propagation approach," in *Proc. IEEE 79th Veh. Technol. Conf. (VTC Spring)*, Seoul, South Korea, May 2014, pp. 1–5.
[48] Y.-M. Chen, C.-F. Lin, and Y.-L. Ueng, "An LDPC-coded generalized space shift keying scheme using a codebook-assisted low-complexity massive MIMO detector," *IEEE Commun. Lett.*, vol. 20, no. 3, pp. 454–457, Mar. 2016.
[49] J. Xu, L. Chen, I. Djurdjevic, S. Lin, and K. Abdel-Ghaffar, "Construction of regular and irregular LDPC codes: Geometry decomposition and masking," *IEEE Trans. Inf. Theory*, vol. 53, no. 1, pp. 121–134, Jan. 2007.
[50] R. Storn and K. Price, "Differential evolution—A simple and efficient heuristic for global optimization over continuous spaces," *J. Global Optim.*, vol. 11, no. 4, pp. 341–359, 1997.

HAN JIN PARK received the B.S., M.S., and Ph.D. degrees in electrical engineering from Chung-Ang University, Seoul, South Korea, in 2012, 2014, and 2023, respectively. From 2016 to 2018, he was with Ims & Nano Tech Company Ltd. From 2018 to 2019, he was with the Institute of Innovative Functional Imaging, Chung-Ang University, Seoul. His current research interests include MIMO systems, iterative soft detection and decoding for wireless communication systems, and coding and information theory.

JEONG WOO LEE (Member, IEEE) received the B.S. and M.S. degrees in electrical engineering from Seoul National University, Seoul, South Korea, in 1994 and 1996, respectively, and the Ph.D. degree in electrical engineering from the University of Illinois at Urbana–Champaign, IL, USA, in 2003.

From 2003 to 2004, he was a Postdoctoral Research Associate with the Coordinated Science Laboratory, Urbana, IL, USA. From 2017 to 2018, he was a Visiting Scholar with UC San Diego, CA, USA. Since 2004, he has been a Professor with the School of Electrical and Electronics Engineering, Chung-Ang University, Seoul. His current research interests include MIMO systems, wireless communications, coding and information theory, and AI-aided communications. From 2016 to 2020, he served as an Associate Editor for *IET Electronics Letters*. He is currently a Guest Editor of *Sensors*. From 2021 to 2022, he served as the Treasurer of the IEEE Seoul Section.